Testing the properties of the QED vacuum, a review
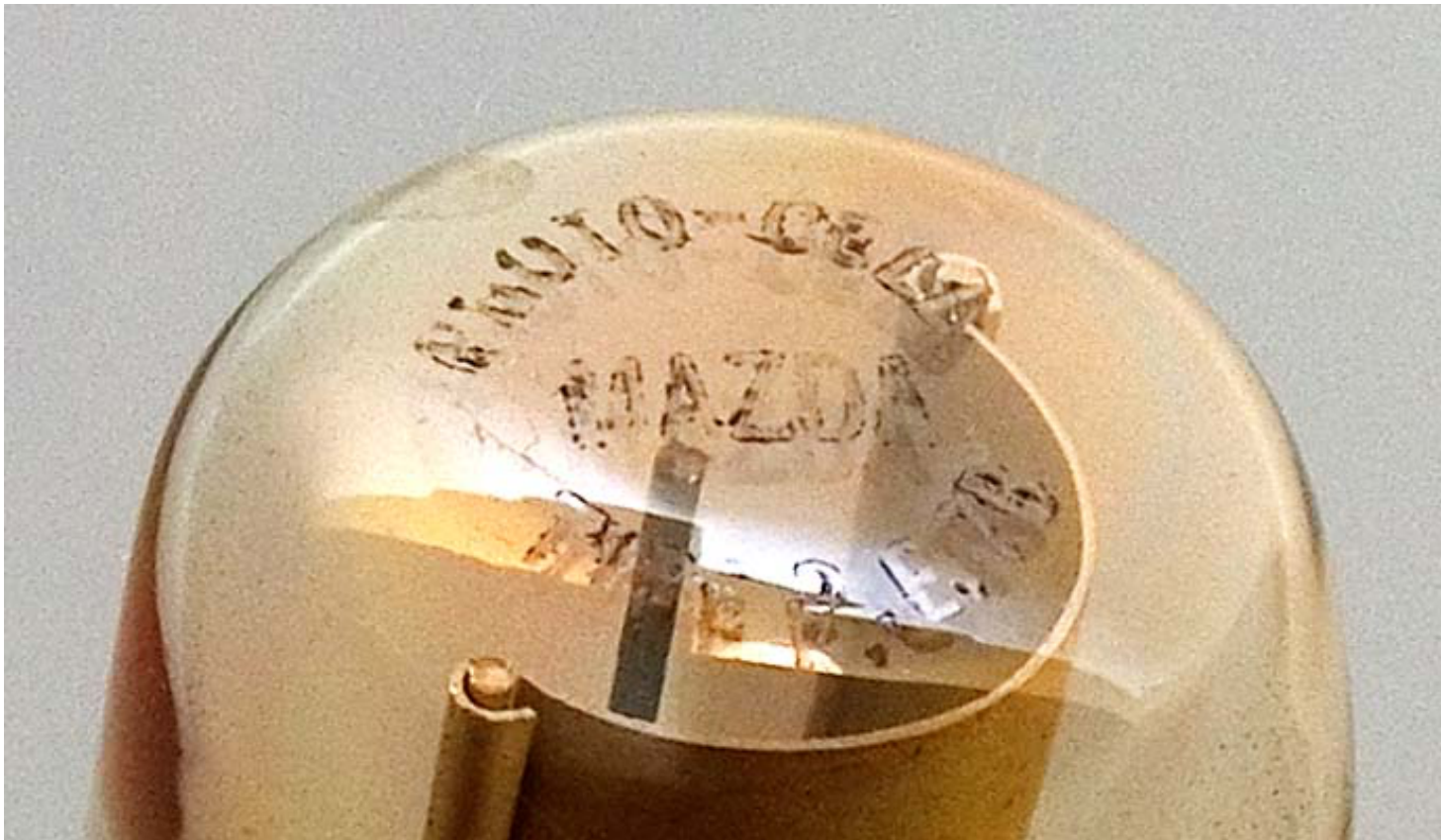
Edoardo Milotti
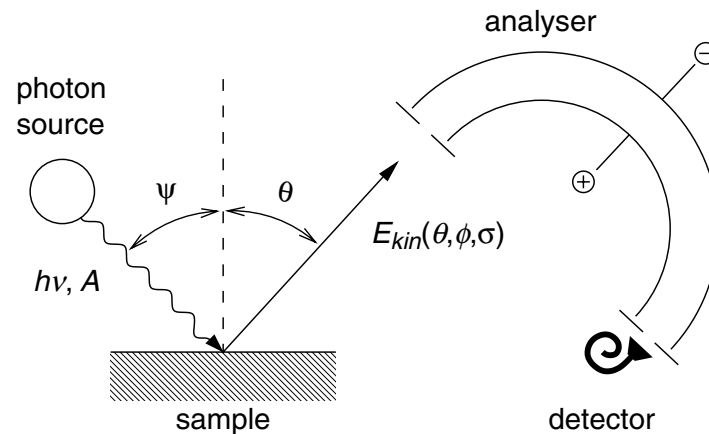
Dipartimento di Fisica, Università di Trieste and INFN - Sezione di Trieste

fppt.com

In the photoelectric effect photons interact with materials and extract photoelectrons ...

detail of an old photocell showing the light-sensitive cathode and the central collecting anode

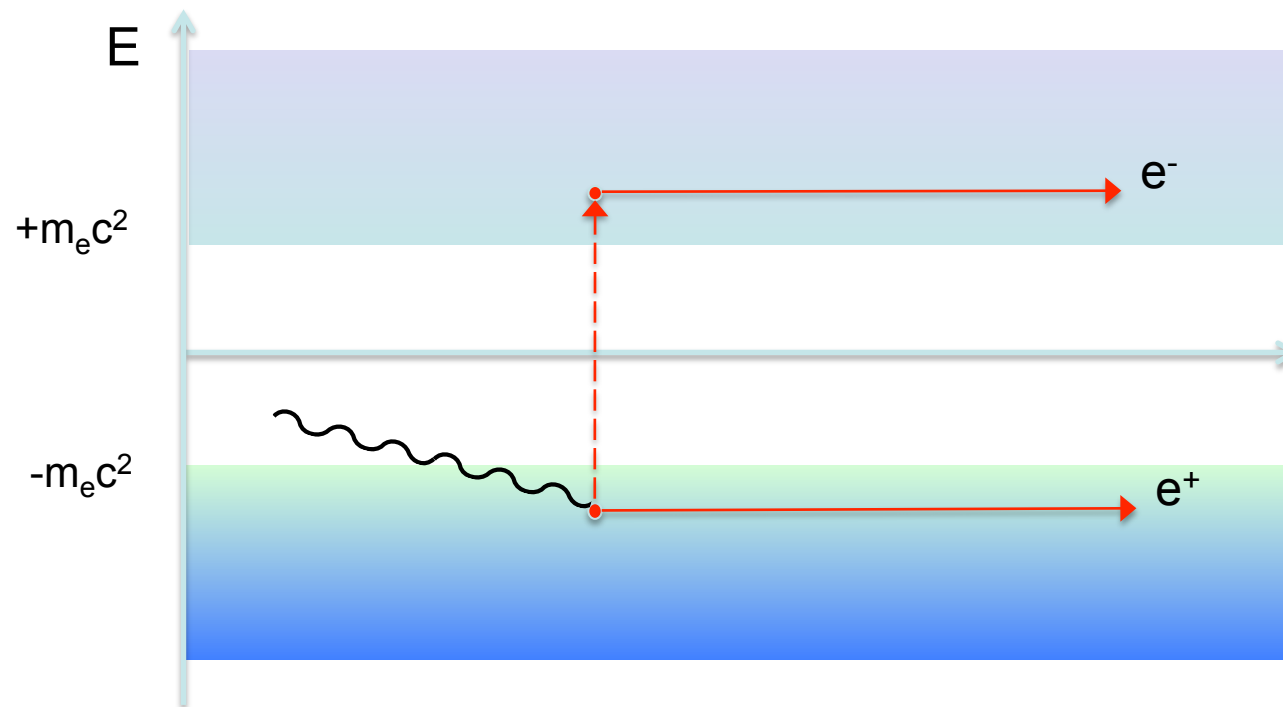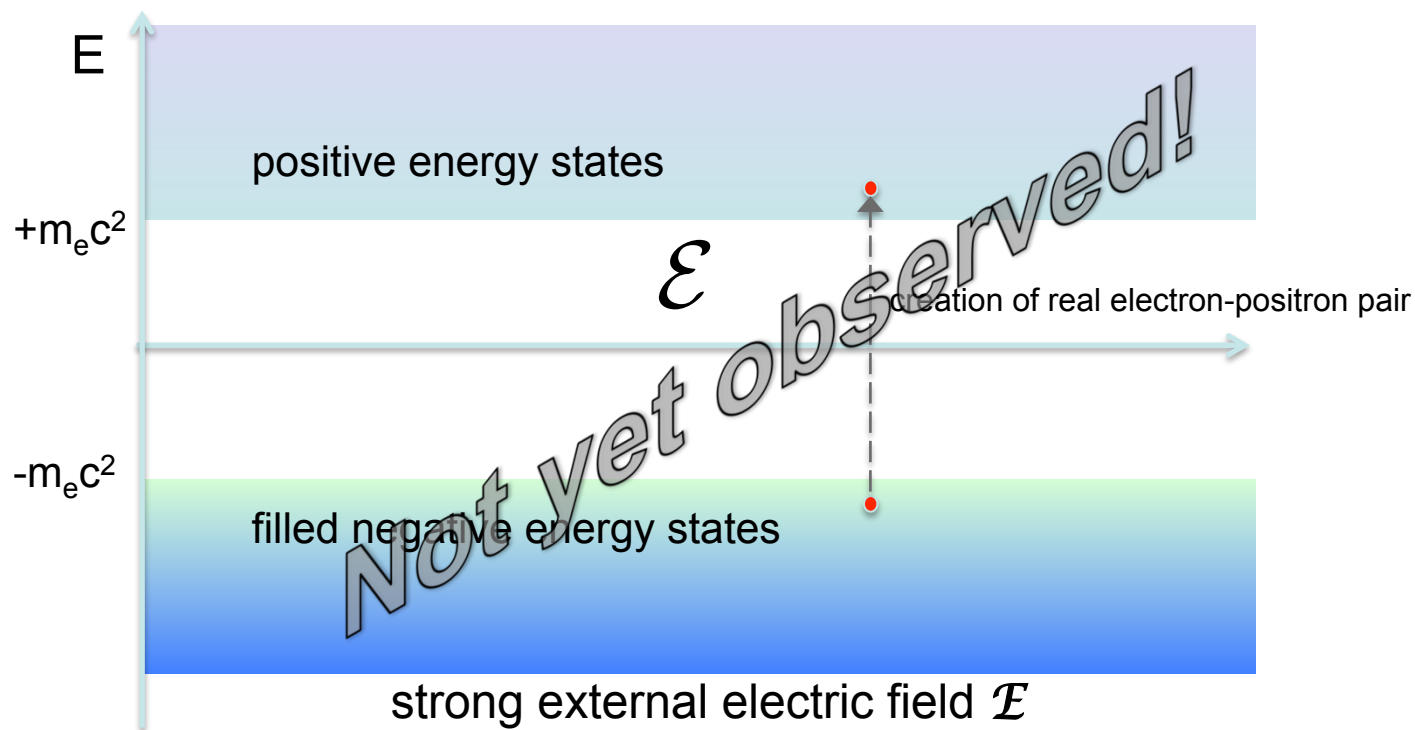## ... and in this way they can be used to study material properties

Principle of a photoemission spectroscopy (PES) experiment

Figure 2. Principle of a modern photoemission spectrometer. Monochromatic photons with energy $h\nu$ and polarization (A is the vector potential of the electromagnetic field) are produced by a light source, e.g. an Al-K_α x-ray anode for XPS or a helium discharge lamp for UPS, and hit the sample surface under an angle Ψ with respect to the surface normal. The kinetic energy E_{kin} of the photoelectrons can be analysed by use of electrostatic analysers (usually by an additional retarding field) as a function of the experimental parameters, e.g. emission angle (θ, ϕ), the electron spin orientation σ, or the photon energy or polarization. The whole setup is evacuated to ultra high vacuum (UHV, typically $p \lesssim 10^{-10}$ mbar).

(from F Reinert and Stefan Hüfner, "Photoemission spectroscopy—from early days to recent applications" New Journal of Physics 7 (2005) 97)

Similarly, photons can interact with the Dirac sea, and extract electrons out of it, just as if it were another material. Since electrons leave a positive charge behind, this creates an electron-positron pair.

E

$+m_e c^2$

e^-

$-m_e c^2$

e^+

E

positive energy states

$+m_e c^2$

$\mathcal{E}$

creation of real electron-positron pair

Not yet observed!

$-m_e c^2$

filled negative energy states

strong external electric field $\mathcal{E}$

Extraction of electron pairs from vacuum under the action of a strong electric field: it can be formalized as a tunnelling effect (Schwinger effect)

Estimate of critical field: *charge separation energy ≈ electron rest energy*

$$eV_c\lambda = e\mathcal{E}_c \frac{\hbar}{mc} \approx mc^2 \qquad \Longrightarrow \qquad \mathcal{E}_c = \frac{m^2 c^3}{e\hbar} \approx 1.3\ 10^{18}\mathrm{V/m}$$

fppt.com
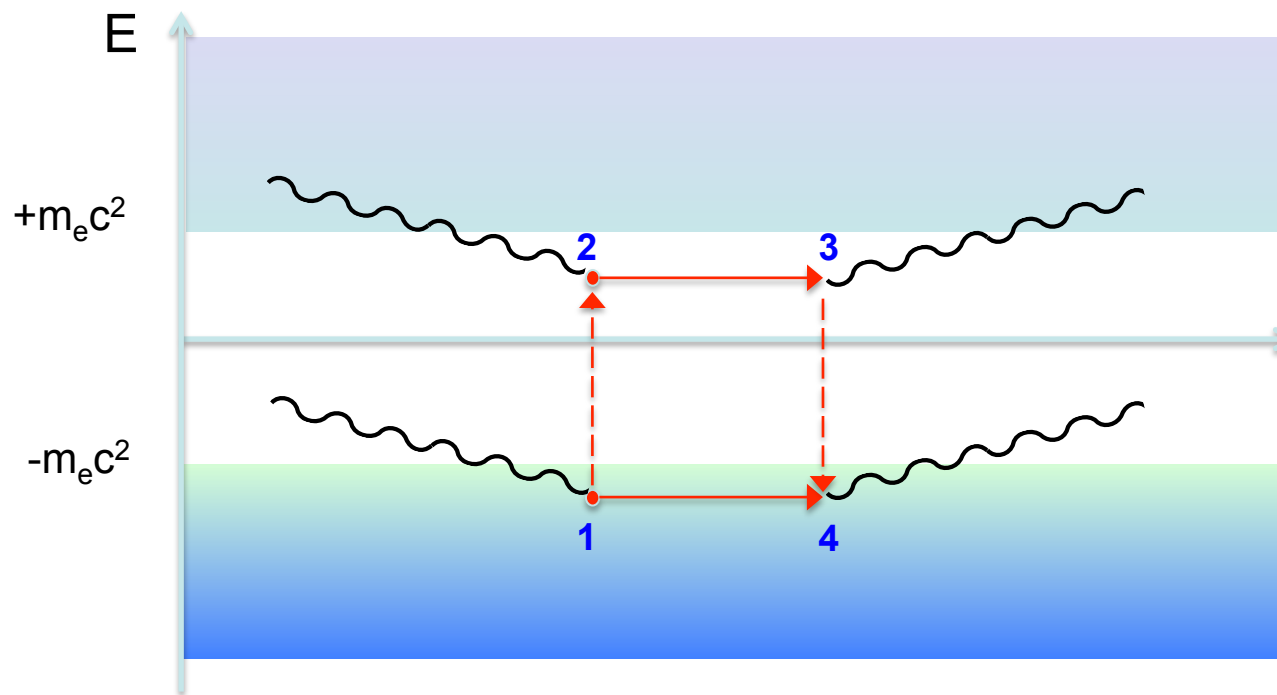
Similarly, when only virtual states are involved, **the process of photon absorption, pair creation, and photon reemission, and corresponds to photon-photon scattering**.

Just as we use photons to study materials, we can use photons to probe the QED vacuum.

**Some early efforts to detect photon-photon scattering
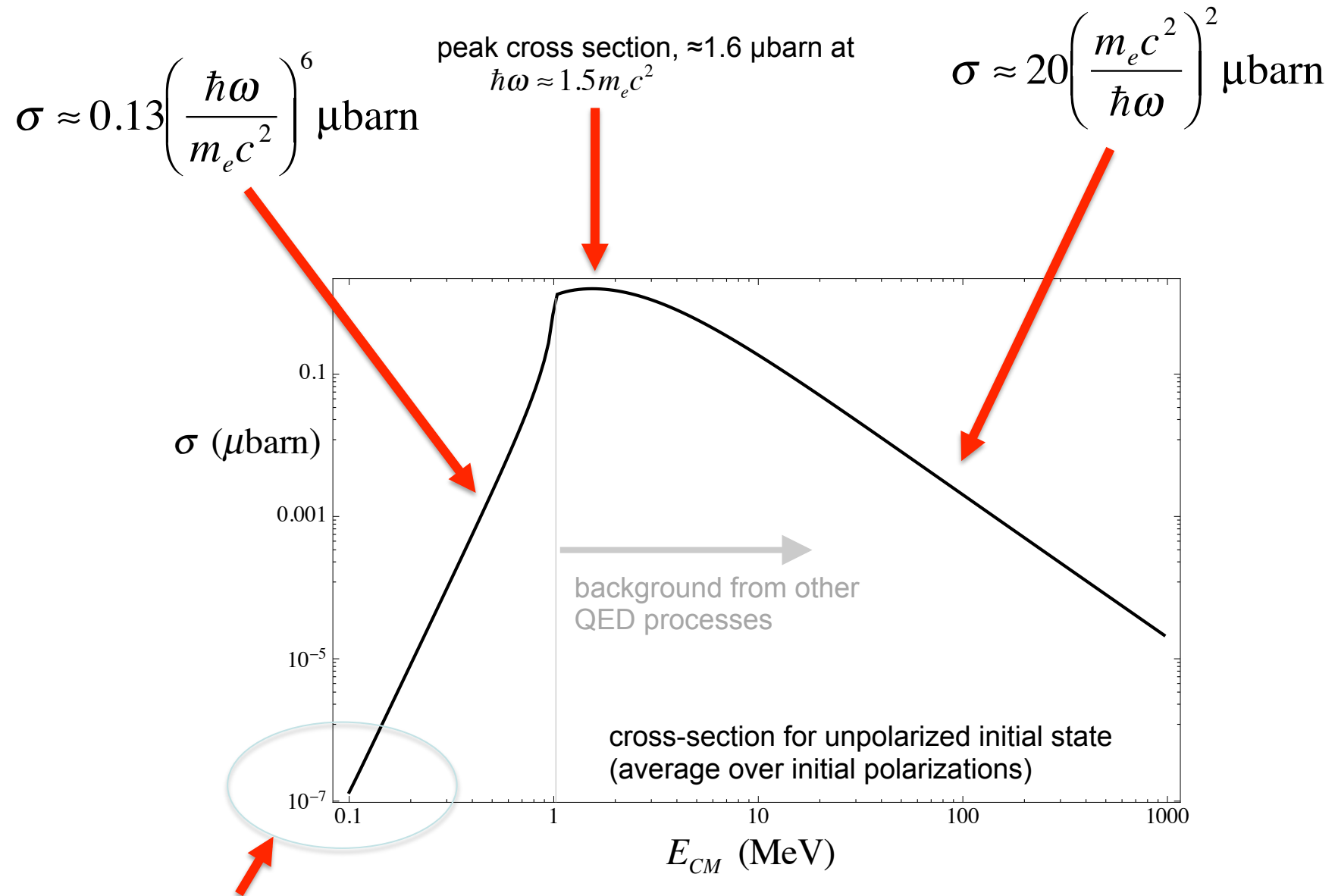(real or virtual photons)**

- Eddy, Morley and Miller – 1898
  - tried to detect the influence of a magnetic field on the velocity of light with a Michelson interferometer and surrounding coils
- Hughes and Jauncey – 1930
  - attempted detection of photons from colliding sunlight
- Watson – 1930
  - attempt to detect the transverse shift of a light beam from magnetic field action
- Farr & Banwell – 1932-1940
  - application of interferometric methods to detect the influence of a magnetic field on the propagation of light

No effect was detected, but this is not surprising, in view of the extremely small photon-photon scattering cross-sectionat visible light energies.

fppt.com
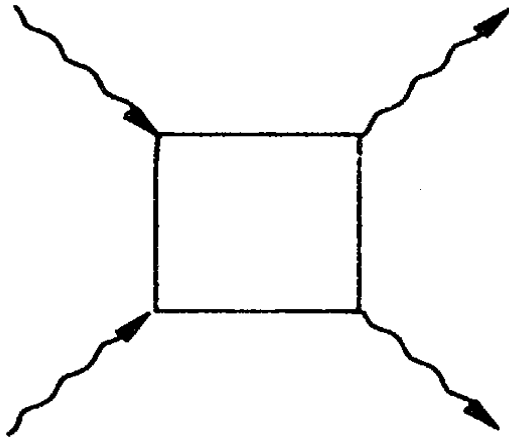
Photon-photon cross section calculations

- **1934**: Breit and Wheeler compute the photon-photon scattering cross-section for energies higher than $2m_e$;
- **1935**: Euler and Kochel provide a first general formula for the photon-photon scattering cross-section also for energies lower than the $2m_e$ threshold;
- **1936**: Euler provides the details of the cross-section formula (work done by Euler for his PhD thesis in Leipzig);
- **1936-37**: Akhiezer, Landau and Pomerancuk generalize the cross-section formula to high energies;
- **1950-51**: Karplus and Neuman carry out a thorough analysis using Feynman diagrams;
- **1964-65**: DeTollis utilizes dispersion relation techniques to give compact formulas for the scattering amplitudes;

$$\sigma \approx 0.13 \left(\frac{\hbar\omega}{m_e c^2} \right)^6 \text{ μbarn}$$

peak cross section, ≈1.6 μbarn at $\hbar\omega \approx 1.5 m_e c^2$

$$\sigma \approx 20 \left(\frac{m_e c^2}{\hbar\omega} \right)^2 \text{ μbarn}$$

σ (μbarn)

background from other QED processes

cross-section for unpolarized initial state (average over initial polarizations)

E_{CM} (MeV)

very low energy region: cross section is extremely small, but photon numbers can be very large here, there is no background from other QED processes, and experimental apparatus is comparatively easier to build

Low-energy effective Lagrangian

Full non-perturbative calculation with uniform background field (Euler, Heisenberg, and Weisskopf), derived from exact solutions of the Dirac equation in constant background electric and magnetic field:

$$\mathcal{L} = \frac{e^2}{hc} \int_0^\infty \frac{d\eta}{\eta^3} e^{-\eta} \left\{ i\eta^2 (\mathbf{E} \cdot \mathbf{B}) \frac{\cos\left(\frac{\eta}{\mathcal{E}_c}\sqrt{\mathbf{E}^2 - \mathbf{B}^2 + 2i(\mathbf{E} \cdot \mathbf{B})}\right) + c.c.}{\cos\left(\frac{\eta}{\mathcal{E}_c}\sqrt{\mathbf{E}^2 - \mathbf{B}^2 + 2i(\mathbf{E} \cdot \mathbf{B})}\right) - c.c.} + \mathcal{E}_c^2 + \frac{\eta^2}{3}(\mathbf{B}^2 - \mathbf{E}^2) \right\}$$

Euler and Heisenberg also produced a simplified form of the effective Lagrangian

$$\mathcal{L} = 4\pi^2 mc^2 \left(\frac{mc}{h}\right)^3 \int_0^\infty \frac{d\eta}{\eta^3} e^{-\eta} \left[-a\eta \cot(a\eta) b\eta \coth(b\eta) + 1 + \frac{\eta^2}{3}(b^2 - a^2) \right]$$

where $\quad a^2 - b^2 = (\mathbf{E}^2 - \mathbf{B}^2)/\mathcal{E}_c^2 \quad$ and $\quad ab = (\mathbf{E} \cdot \mathbf{B})/\mathcal{E}_c^2$

"proper time" variable (fully developed later by Stückelberg, Feynman and Schwinger)

subtraction of the infinite free-field effective action

this corresponds to a log term in the integrated Lagrangian: it is an embryonic form of charge renormalization

$$\mathcal{L} = 4\pi^2 mc^2 \left(\frac{mc}{h}\right)^3 \int_0^\infty \frac{d\eta}{\eta^3} e^{-\eta} \left[-a\eta \cot(a\eta) b\eta \coth(b\eta) + 1 + \frac{\eta^2}{3}(b^2 - a^2) \right]$$

where $\quad a^2 - b^2 = (\mathbf{E}^2 - \mathbf{B}^2)/\mathcal{E}_c^2 \quad$ and $\quad ab = (\mathbf{E} \cdot \mathbf{B})/\mathcal{E}_c^2$

scalar invariant

pseudoscalar invariant related to axial symmetry

The lowest-order expansion of the HE Lagrangian yields

$$\mathcal{L} = -\mathcal{F} + \frac{8\alpha^2}{45m_e^4}\mathcal{F}^2 + \frac{14\alpha^2}{45m_e^4}\mathcal{G}^2$$

$$= -\frac{1}{2}(\mathbf{E}^2 - \mathbf{B}^2) + \frac{2\alpha^2}{45m_e^4}\left[(\mathbf{E}^2 - \mathbf{B}^2)^2 + 7(\mathbf{E}\cdot\mathbf{B})^2\right]$$

where $\quad \mathcal{F} = \frac{1}{4}F_{\mu\nu}F^{\mu\nu} = \frac{1}{2}(\mathbf{E}^2 - \mathbf{B}^2); \quad \mathcal{G} = \frac{1}{4}F_{\mu\nu}\tilde{F}^{\mu\nu} = \mathbf{E}\cdot\mathbf{B}$

or also (SI units)

$$\mathcal{L}_{HE} = \frac{A_e}{\mu_0}\left[\left(\frac{\mathbf{E}^2}{c^2} - \mathbf{B}^2\right)^2 + 7\left(\frac{\mathbf{E}}{c}\cdot\mathbf{B}\right)^2\right] \qquad \text{where} \quad A_e = \frac{2\alpha^2 \lambdabar_e^3}{45\mu_0 m_e c^2} \approx 1.32\ 10^{-24}\ \text{T}^{-2}$$

The optical properties of QED vacuum can be derived from the effective EHW Lagragian

The equation of motion of the fields is

$$0 = \partial_\mu \left(F^{\mu\nu} - \frac{4\alpha^2}{45 m_e^4} F^{\alpha\beta} F_{\alpha\beta} F^{\mu\nu} - \frac{7\alpha^2}{45 m_e^4} F^{\alpha\beta} F_{\alpha\beta} \tilde{F}^{\mu\nu} \right)$$

or, equivalently,

$$\mathbf{D} = \frac{1}{\epsilon_0} \frac{\partial \mathcal{L}}{\partial \mathbf{E}}; \quad \mathbf{H} = -\mu_0 \frac{\partial \mathcal{L}}{\partial \mathbf{B}}$$

and these equations yield effective values for the electrical and magnetic polarizabilities,

$$\varepsilon_{ij} \approx \delta_{ij} + \frac{4\alpha^2}{45 m^4} \left[2 \left(\mathbf{E}^2 - \mathbf{B}^2 \right) \delta_{ij} + 7 B_i B_j \right]; \qquad \mu_{ij} \approx \delta_{ij} + \frac{4\alpha^2}{45 m^4} \left[2 \left(\mathbf{B}^2 - \mathbf{E}^2 \right) \delta_{ij} + 7 E_i E_j \right]$$

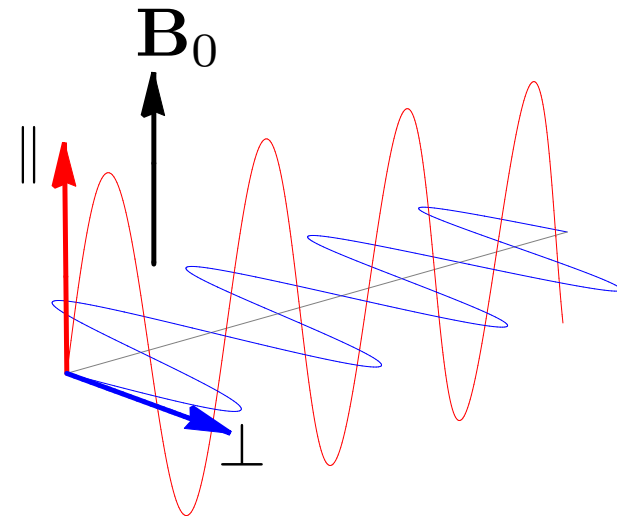Then, assuming that light propagates in a uniform, dipolar magnetic field $\mathbf{B}_0$, we find

$$n_\parallel = 1 + 7 A_e B_0^2$$

$$n_\perp = 1 + 4 A_e B_0^2$$

and eventually

$$\Delta n = n_\parallel - n_\perp = 3 A_e B_0^2$$

so that the magnetized vacuum of QED is birefringent.

fppt.com

We can associate this result to the critical fields

critical magnetic field from the critical electric field

$$\mathcal{E}_c = \frac{m^2 c^3}{e\hbar} \approx 1.3 \ 10^{18} \ \text{V/m} \quad \Rightarrow \quad \mathcal{B}_c = \frac{\mathcal{E}_c}{c} = \frac{m^2 c^2}{e\hbar} \approx 4.4 \ 10^9 \ \text{T}$$

then

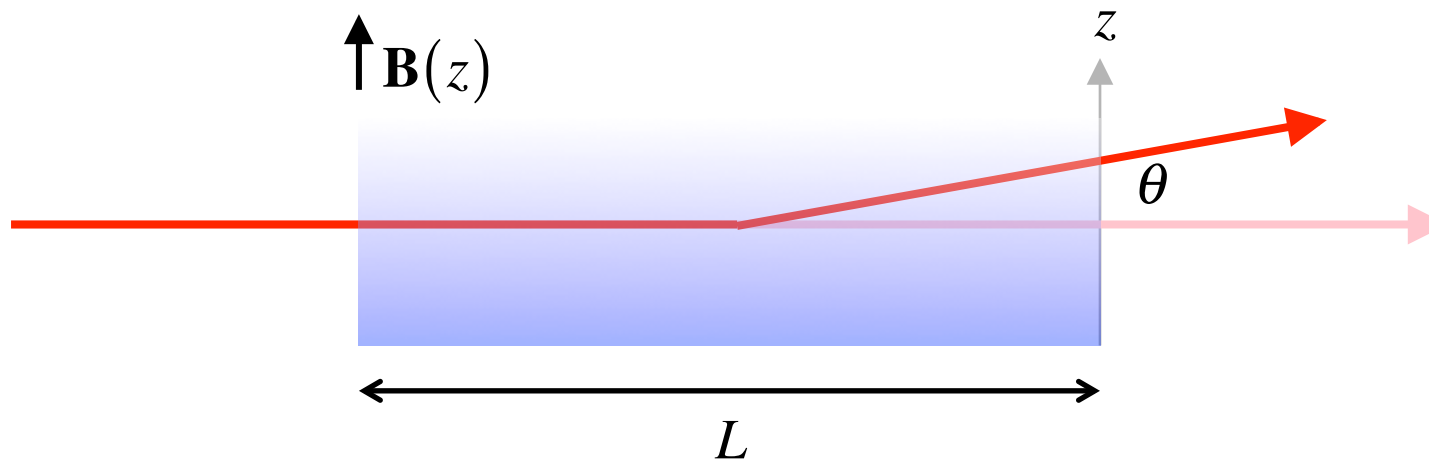$$A_e = \frac{\alpha}{90\pi} \left(\frac{1}{\mathcal{B}_c^2} \right)$$

and

$$\Delta n = 3 A_e B_0^2 = \frac{\alpha}{30\pi} \left(\frac{B}{\mathcal{B}_c} \right)^2 \approx 7.7 \ 10^{-5} \left(\frac{B}{\mathcal{B}_c} \right)^2$$

$$\Delta n \big|_{B=2.5 \ \text{T}} \approx 2.5 \ 10^{-23}$$

It is extremely difficult to measure such a small refractive index difference.

Consider for instance what happens with a strong magnetic field gradient, which induces a refractive index gradient.

$$\uparrow \mathbf{B}(z)$$

$$z$$

$$\theta$$

$$L$$

QED prediction

$$\Delta n \approx \left(4 \cdot 10^{-24} \ \mathrm{T}^{-2}\right) B^2$$

Deflection due to a refractive index gradient

$$\theta \approx \frac{1}{n}\frac{\partial n}{\partial z}L \approx \left(8 \cdot 10^{-24} \ \mathrm{T}^{-2}\right) B \frac{\partial B}{\partial z} L$$

$$\theta \approx 10^{-19} \ \mathrm{radians}$$

with $L \approx 10000$ ly; $\qquad B\frac{\partial B}{\partial z} \approx \left(10^{-6} \ \mathrm{T}\right) \cdot \left(10^{-9} \ \mathrm{T/m}\right)$

Over the years several experimental proposals have been put forward to observe photon photon scattering and QED-induced optical effects

One early list was compiled by Paul L. Csonka at CERN (see also Phys. Lett. **24B** (1967) 625)

CERN 67-15
Theoretical Study
Division
11 May 1967

ARE PHOTON-PHOTON SCATTERING EXPERIMENTS FEASIBLE ?

Paul L. Csonka
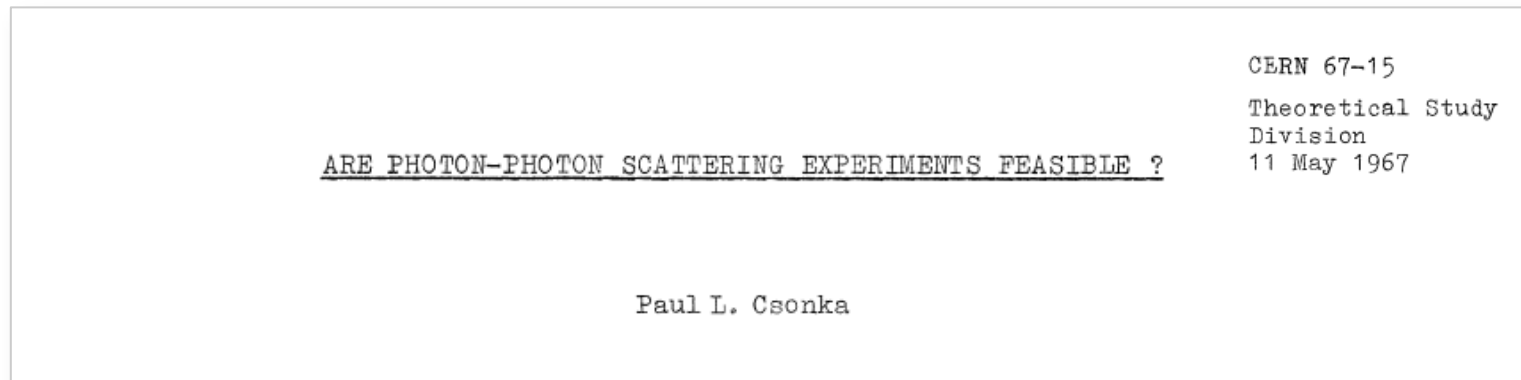
At low energy:

- laser beam clashing with high-energy gamma ray beam
- flash X-ray machines
- nuclear explosions
- synchrotron radiation

The list does not include birefringence measurements in the optical domain. **Moreover, nowadays one must also include photon-photon scattering with high-intensity lasers.**
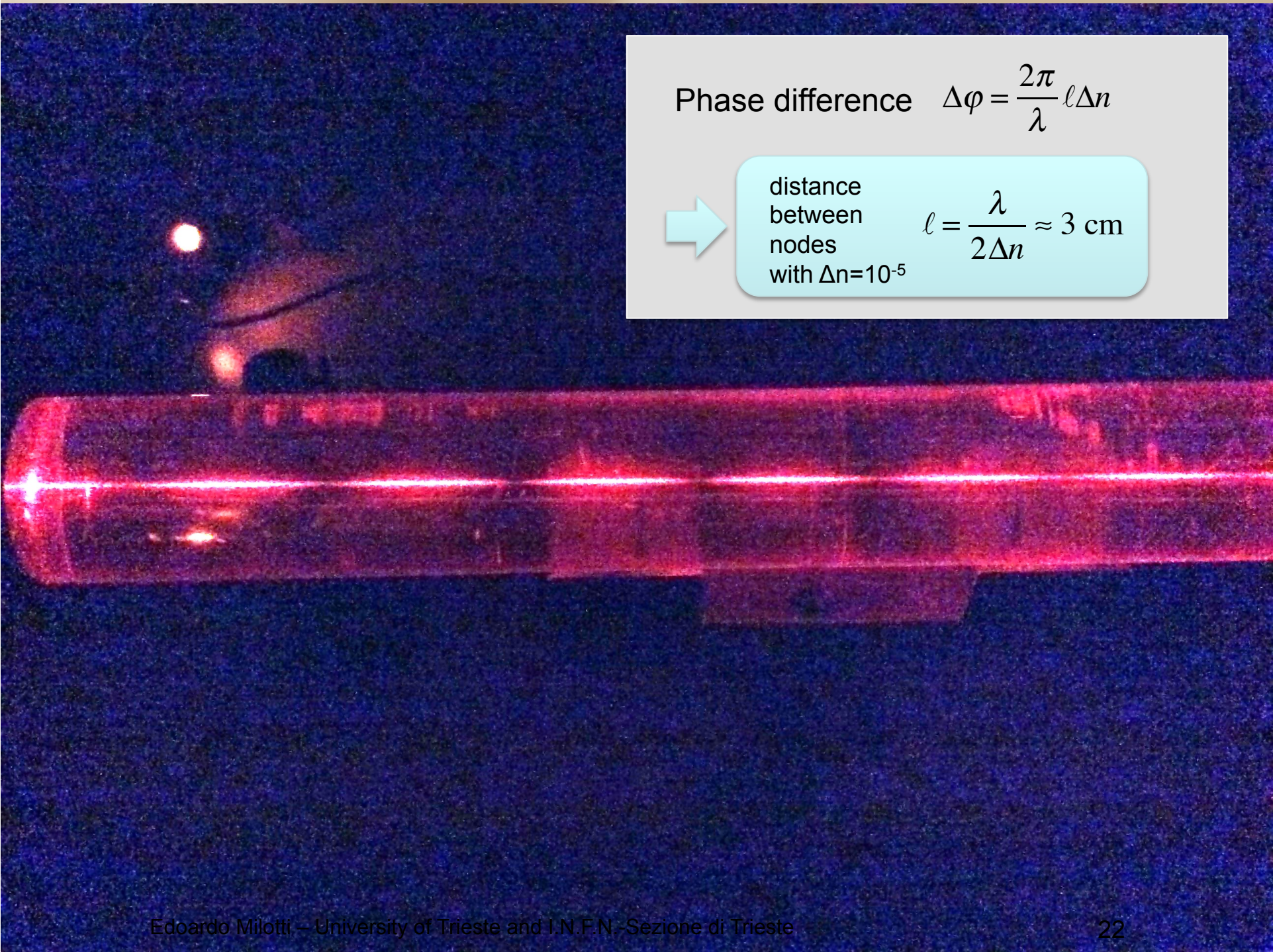
Visualization of the propagation of linearly polarized light in a uniaxial birefringent medium

LASER

linear
polarizer

plexiglas bar

y

LASER
polarization

x

optical axes
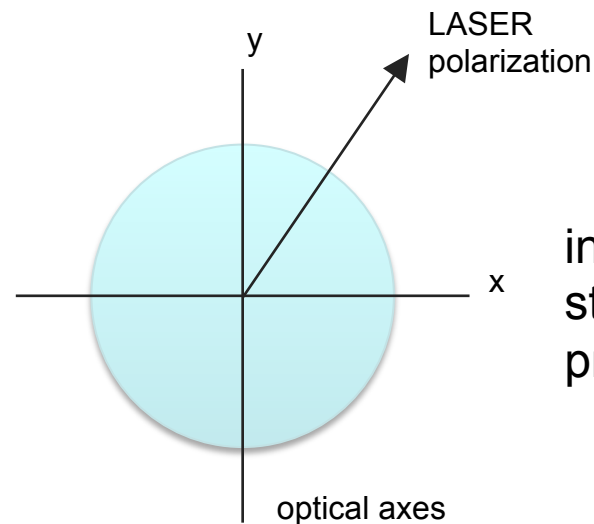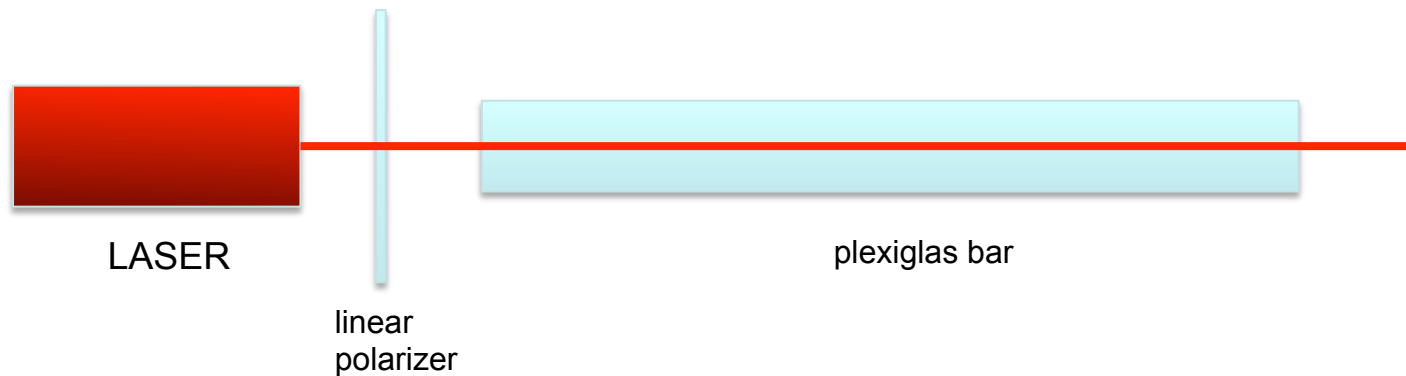
in these conditions the polarization state changes as the LASER light propagates along the bar

21
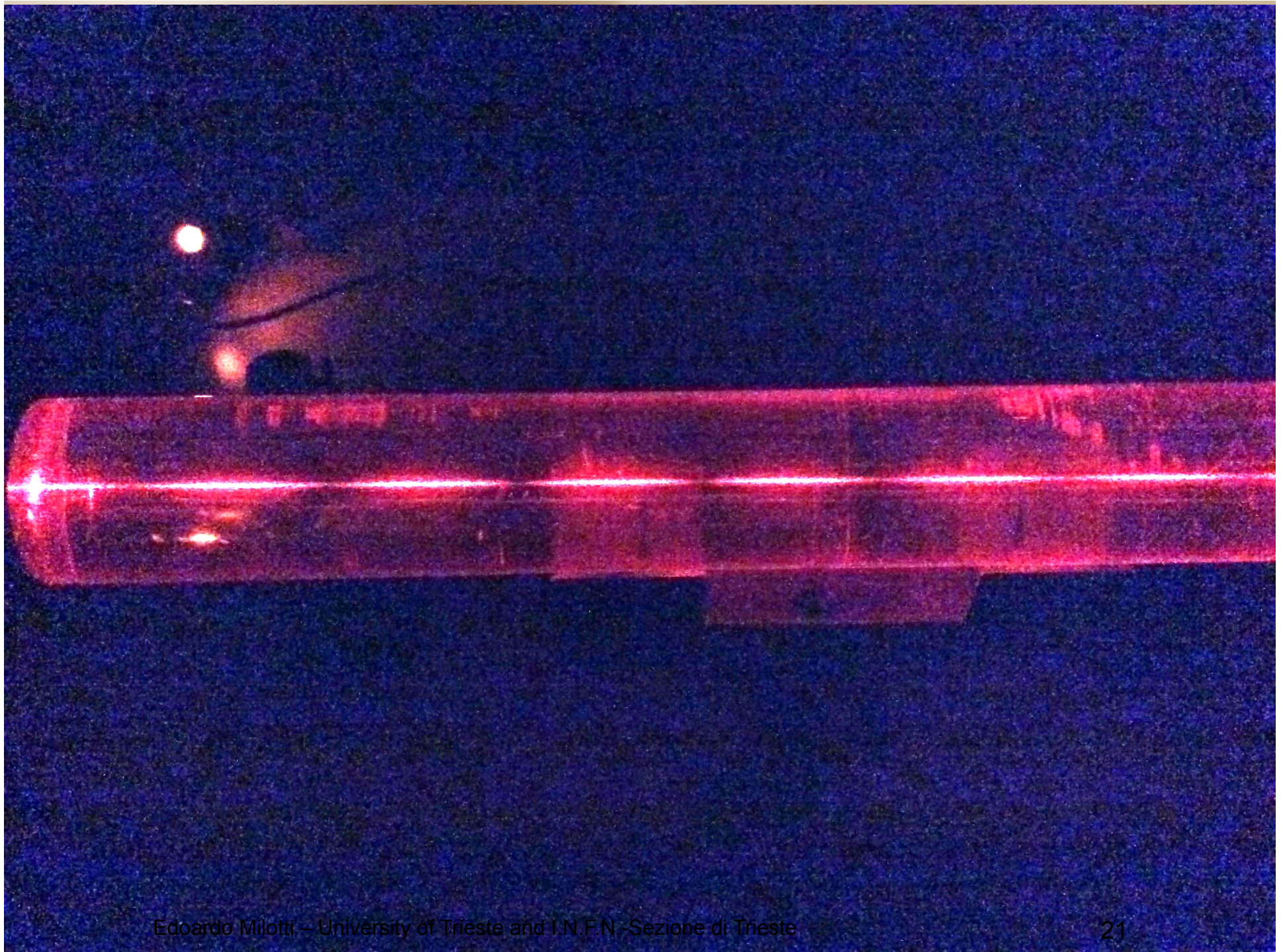
Phase difference $\Delta\varphi = \dfrac{2\pi}{\lambda}\ell\Delta n$

distance between nodes with $\Delta n = 10^{-5}$

$\ell = \dfrac{\lambda}{2\Delta n} \approx 3 \text{ cm}$

In PVLAS there is a similar effect, but

distance between nodes with $\Delta n = 10^{-23}$

$$\ell \approx 3 \cdot 10^{16} \text{ m} \approx 3 \text{ ly}$$

The QED effect is MUCH smaller than the birefringence of plexiglas, and when you try to detect it you have to

- increase the magnetic field as much as possible (remember that it is proportional to $\mathbf{B}^2$)

- **increase the optical path length as much as possible (you fold the light path – and you have the choice between a non resonant multipass cavity and a resonant cavity, a Fabry-Perot interferometer)**

- modulate the physical signal to beat noise

- understand systematic effects and reduce them as much as possible

fppt.com

The search for the birefringence of vacuum

- Jones – 1960
  - used the scheme of the optical lever and a magnetic wedge to attempt to detect spatial changes of the index of refraction of vacuum in the presence of a strong magnetic field gradient
- Erber– 1961
  - reviewed the experimental efforts and stressed the main experimental difficulties

fppt.com

The PVLAS experiment: started back at CERN in the '80's

EUROPEAN ORGANIZATION FOR NUCLEAR RESEARCH

Proposal D2
9 June 1980

EXPERIMENTAL DETERMINATION OF VACUUM POLARIZATION EFFECTS
ON A LASER LIGHT-BEAM PROPAGATING IN A STRONG MAGNETIC FIELD

E. Iacopini, P. Lazeyras, M. Morpurgo, E. Picasso,
B. Smith and E. Zavattini

CERN, Geneva, Switzerland

and

E. Polacco

Università di Pisa, Italy

Zavattini's first try at CERN in 1979-1983

First realization of a prototype apparatus
Delay line optical cavity with modulated magnet

636   J. Opt. Soc. Am. B/Vol. 1, No. 4/August 1984   Carusotto *et al.*
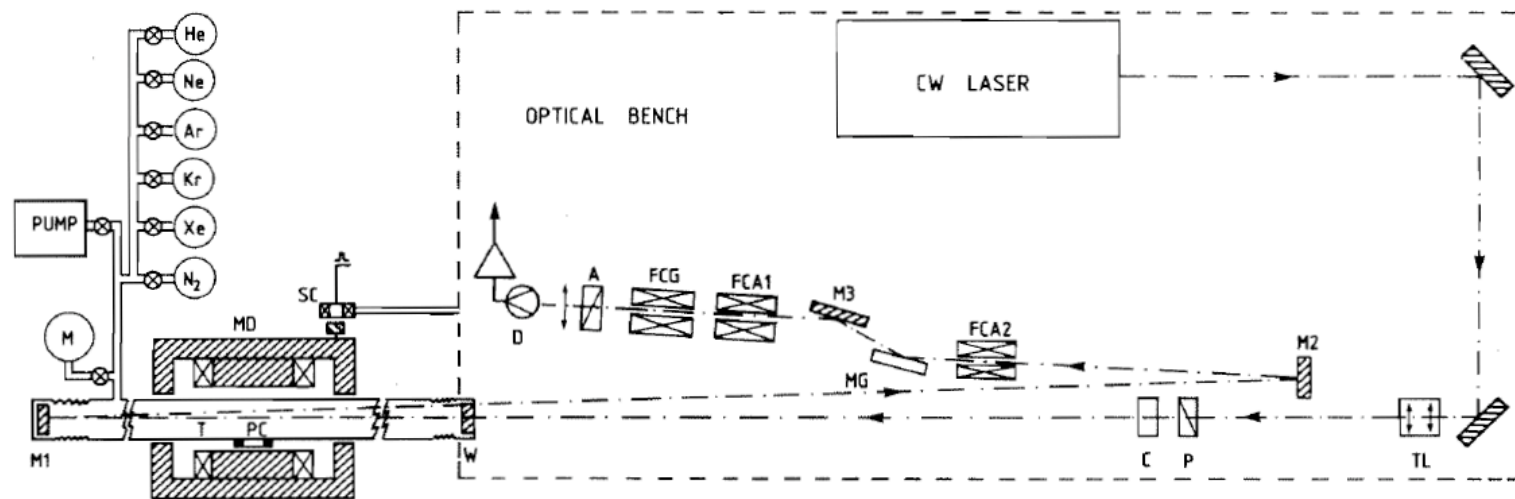
Fig. 1.   Experimental apparatus: optical layout. A, analyzer prism; C, compensator; FCA1 and FCA2, air Faraday cells; FCG, glass Faraday modulator; MG, gold mirror; M3, aluminium mirror; P, polarizer prism; D, photodiode; SC, synchronizing coil; TL, telescope; W, window; M, manometer; MD, rotating dipole magnet; PC, pickup coil.
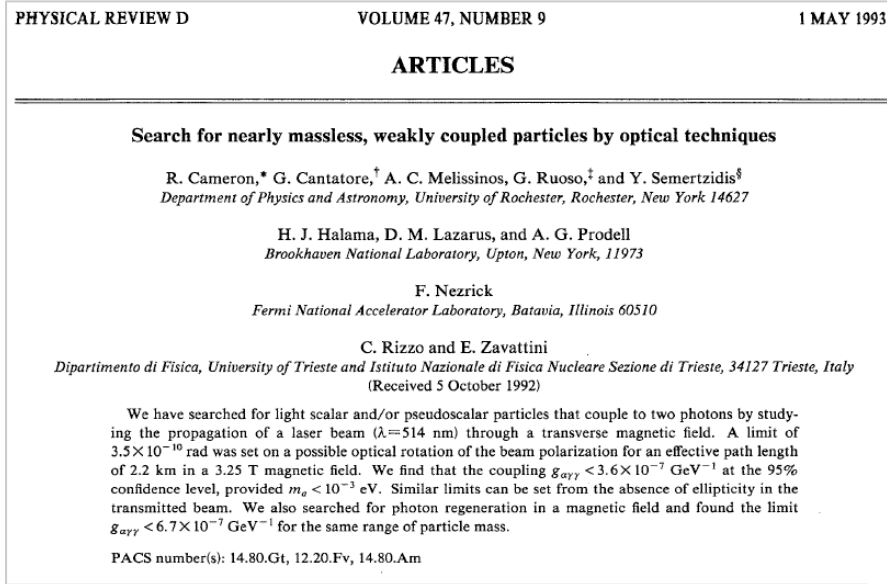
S Carusotto, E Iacopini, E Polacco, F Scuri, G Stefanini, and **E Zavattini**, JOSA B (1984)

Sensitivity not sufficient for vacuum measurement
Obtained result on magnetic polarizability of gases
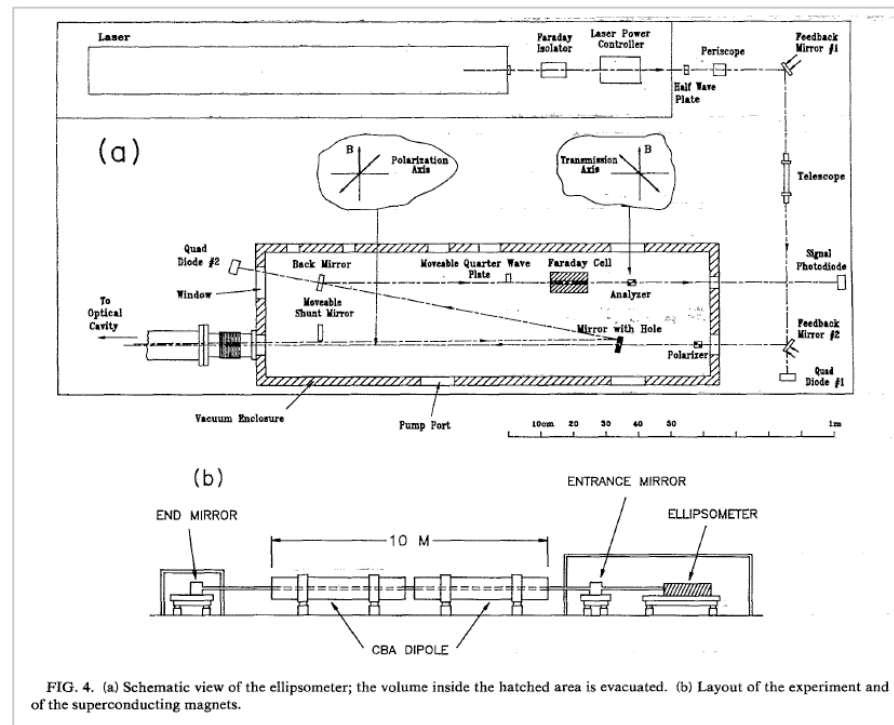
The BNL experiment, 1988-1992

BNL - AGS E840 - LAS

- 4 T maximum magnetic field on two 4.4 m long magnets
- 15 m long delay line optical cavity
- Field amplitude modulated @ tens of mHz

ARTICLES

Search for nearly massless, weakly coupled particles by optical techniques

R. Cameron,* G. Cantatore,† A. C. Melissinos, G. Ruoso,‡ and Y. Semertzidis§
Department of Physics and Astronomy, University of Rochester, Rochester, New York 14627

H. J. Halama, D. M. Lazarus, and A. G. Prodell
Brookhaven National Laboratory, Upton, New York, 11973

F. Nezrick
Fermi National Accelerator Laboratory, Batavia, Illinois 60510

C. Rizzo and E. Zavattini
Dipartimento di Fisica, University of Trieste and Istituto Nazionale di Fisica Nucleare Sezione di Trieste, 34127 Trieste, Italy
(Received 5 October 1992)

We have searched for light scalar and/or pseudoscalar particles that couple to two photons by studying the propagation of a laser beam ($\lambda = 514$ nm) through a transverse magnetic field. A limit of 3.5×10^{-10} rad was set on a possible optical rotation of the beam polarization for an effective path length of 2.2 km in a 3.25 T magnetic field. We find that the coupling $g_{a\gamma\gamma} < 3.6 \times 10^{-7}$ GeV^{-1} at the 95% confidence level, provided $m_a < 10^{-3}$ eV. Similar limits can be set from the absence of ellipticity in the transmitted beam. We also searched for photon regeneration in a magnetic field and found the limit $g_{a\gamma\gamma} < 6.7 \times 10^{-7}$ GeV^{-1} for the same range of particle mass.

PACS number(s): 14.80.Gt, 12.20.Fv, 14.80.Am

Results:

- No good signal detected
- Limits on the coupling constant of light scalar/pseudoscalar particles to two photons

FIG. 4. (a) Schematic view of the ellipsometer; the volume inside the hatched area is evacuated. (b) Layout of the experiment and of the superconducting magnets.
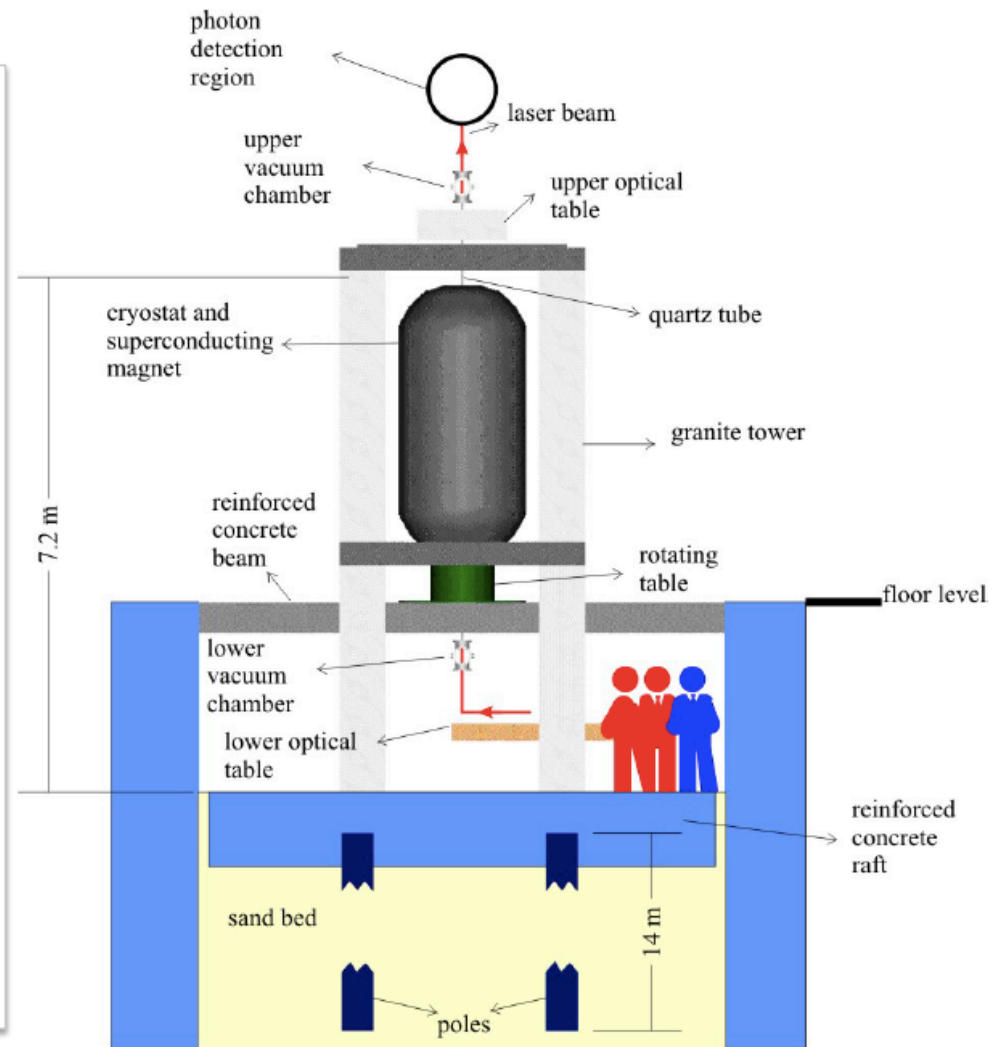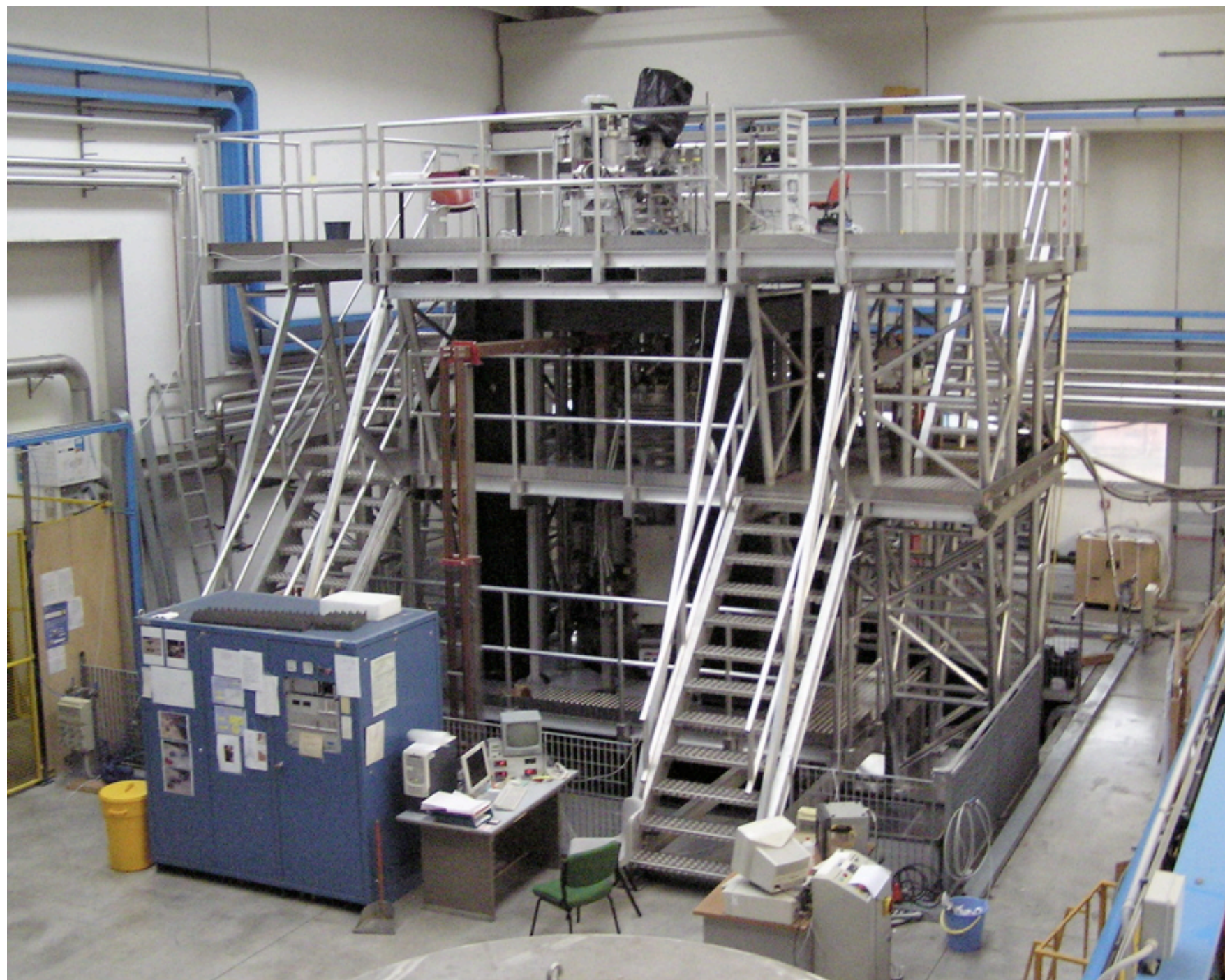
PVLAS at Legnaro, 1992-2008

Polarizzazione del Vuoto con LASer

Major improvements:

• Resonant **FP cavity (6.4 m)** for large amplification factor (> 5 10^4)

• Rotating cryostat allows high modulation frequency (up to 0.4 Hz)

• Large magnetic field (up to 6 T)

• Magnetic system mechanically decoupled from optical system

At present the PVLAS experiment is located in a clean room inside the Physics Dept. of the University of Ferrara

the PVLAS collaboration

- **F. Della Valle**, University of Trieste and INFN-Trieste,
- **A. Ejlli**, University of Ferrara and INFN-Ferrara,
- **U. Gastaldi**, University of Ferrara and INFN-Ferrara,
- **G. Messineo**, University of Ferrara and INFN-Ferrara,
- **E. Milotti**, University of Trieste and INFN-Trieste,
- **R. Pengo**, Laboratori Nazionali di Legnaro – INFN
- **L. Piemontese**, University of Ferrara and INFN-Ferrara,
- **G. Ruoso**, Laboratori Nazionali di Legnaro – INFN
- **G. Zavattini**, University of Ferrara and INFN-Ferrara

The clean room in Ferrara

- Clean room class 10000
- Possible temperature stability system
- Environment with human noise sources during day

The optical table - 1

Actively isolated granite optical bench

4.8 m length, 1.2 m wide, 0.4 m height, 4.5 tons

Compressed air stabilization system for six degrees of freedom Resonance frequency down to 1 Hz

The optical table - 2

The vacuum system

Vacuum chambers

- All components of the vacuum system and optical mounts constructed with **non magnetic materials**

- Vacuum pipe through magnets made of **borosilicate glass** to avoid eddy currents

Linear translator

- Motion of optical components inside vacuum chamber by means of **piezo-motor actuators**

- Low pressure pumping by using getter - NEG pumps – **noise free, magnetic field free**
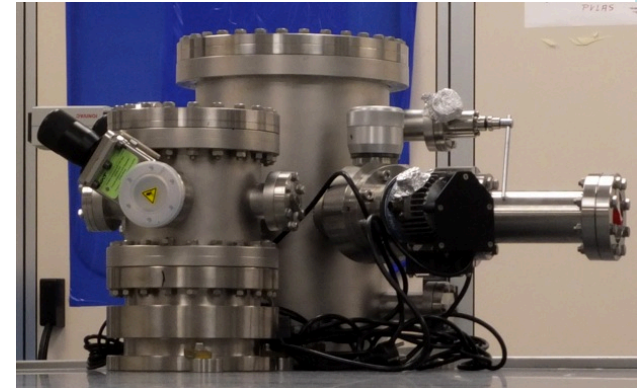
Getter pumps
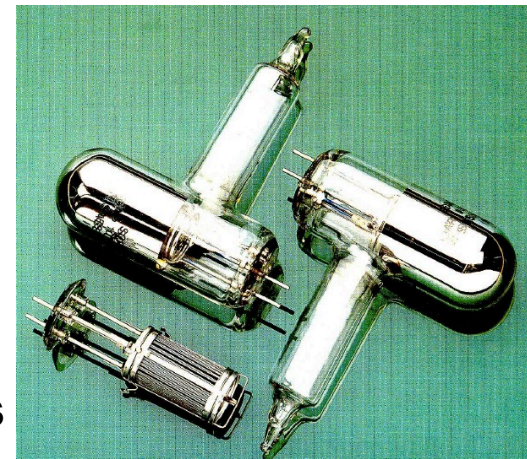
The permanent magnets

Halbach configuration

Total field integral = 10.0 T² m
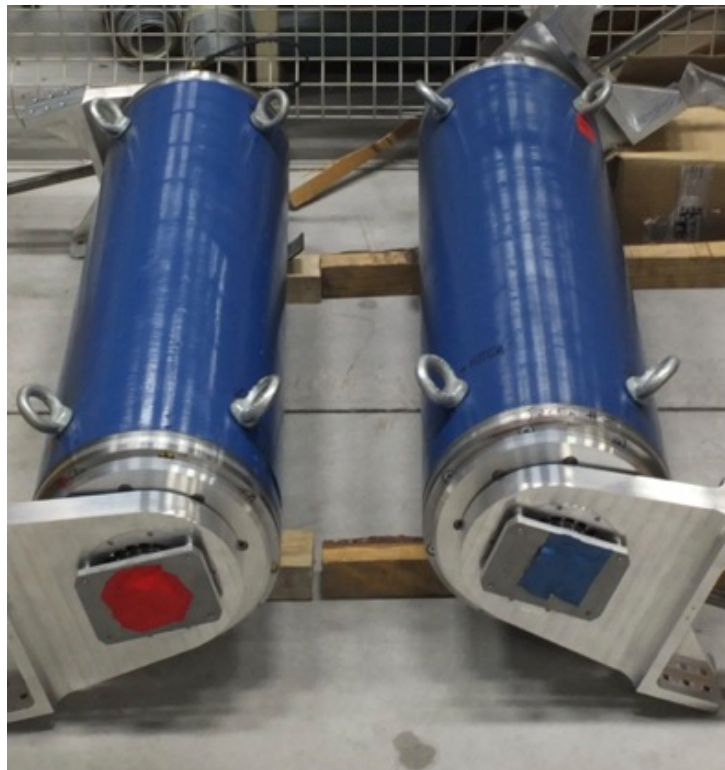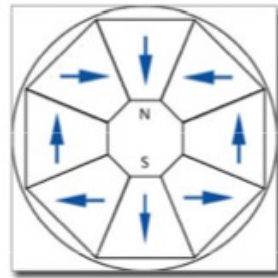
Magnets have built in **magnetic shielding**
Stray field < 1 Gauss on outer surface

$$\triangle n = 2.5 \cdot 10^{-23} \text{ for } B = 2.5 \text{ T}$$

0.9 m

4.8 m
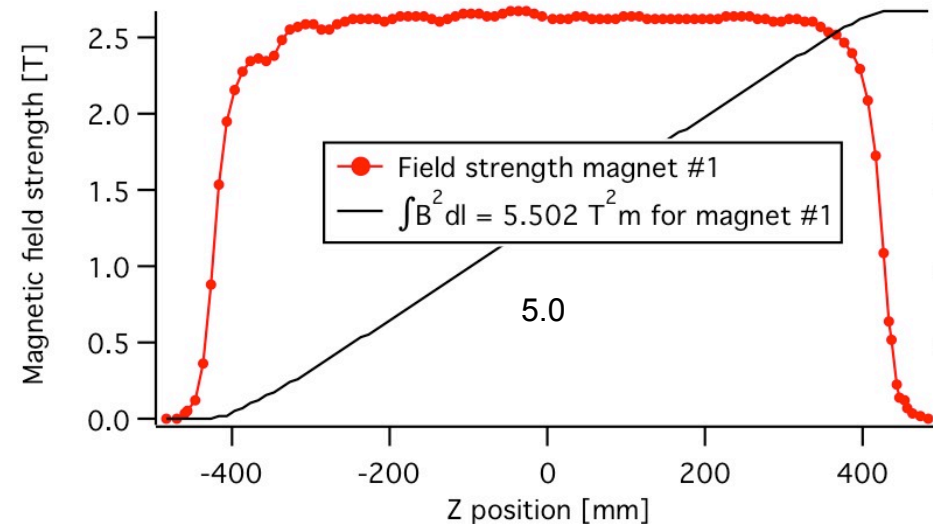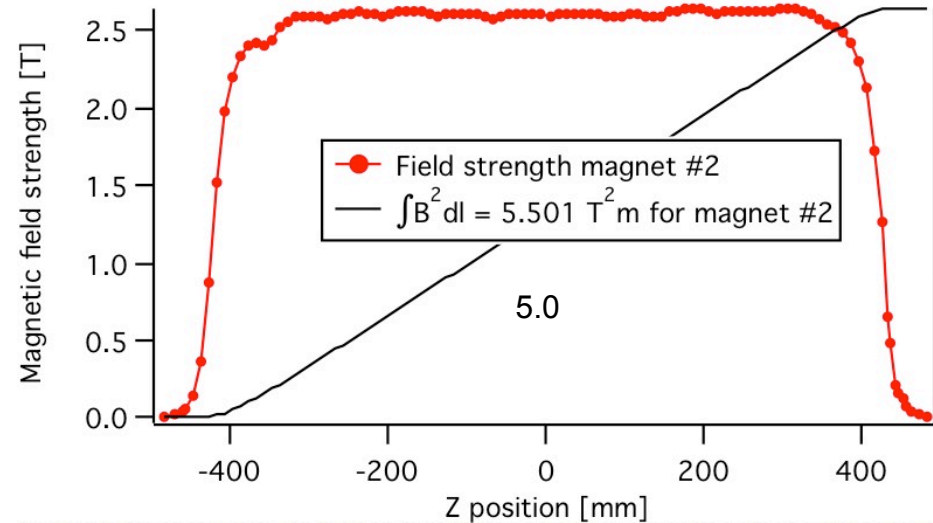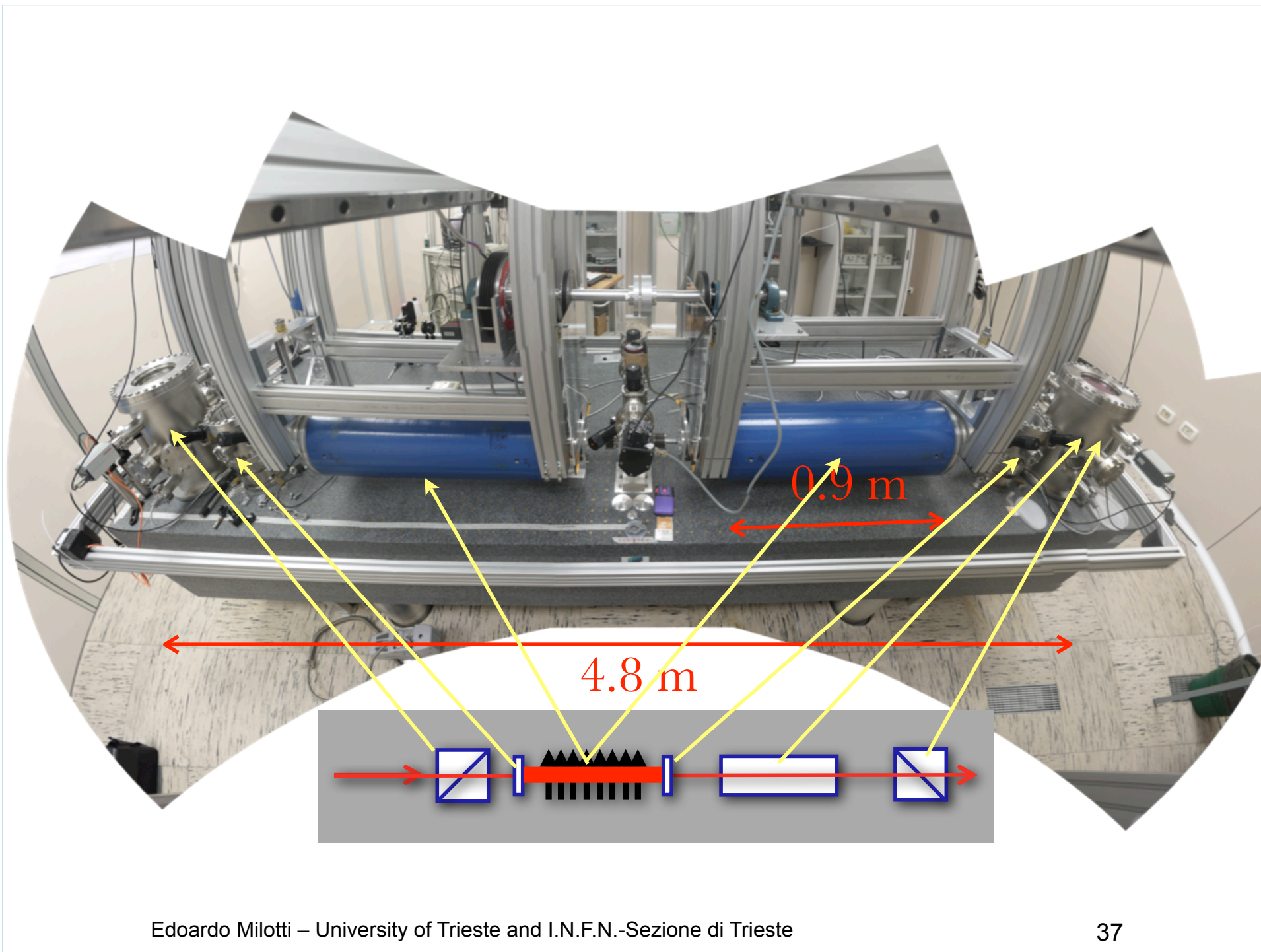
The Fabry-Perot resonator
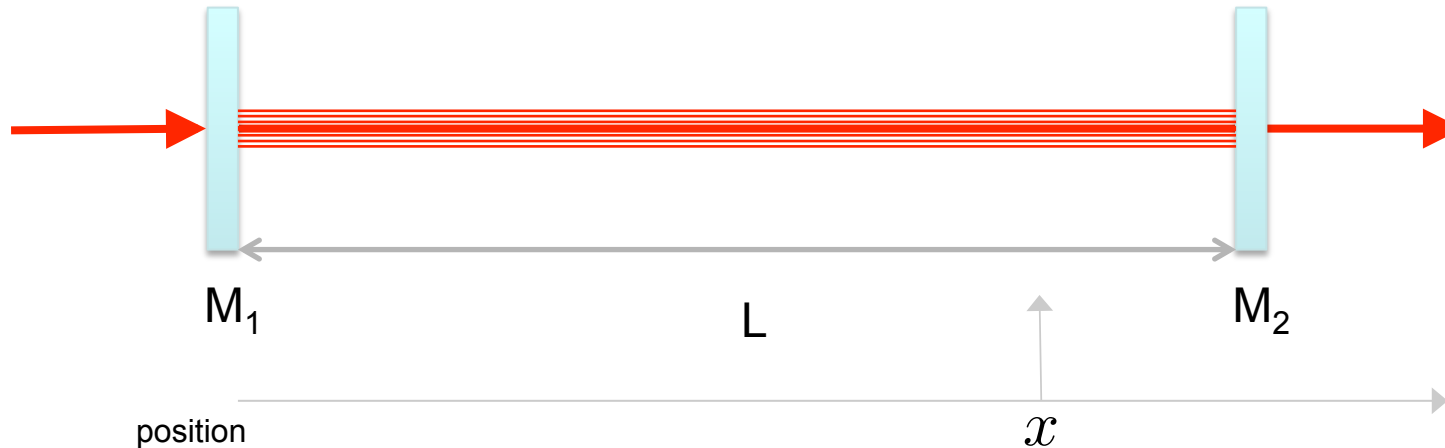
The dynamics of the Fabry-Perot (FP) resonator can be described by a delay equation for the forward-propagating electric field in the resonator

transmittivity of input mirror

mirror reflectivities

$$E_+(t,x) = \mathcal{T}_1 E_{in}(t,x) + \mathcal{R}_1 \mathcal{R}_2 E_+\left(t - \frac{2L}{c}, x\right)$$

forward-propagating electric field in the resonator

incoming field

The delay equation can be solved with a Fourier Transform technique

$$E_+(t,x) = \mathcal{T}_1 E_{in}(t,x) + \mathcal{R}_1 \mathcal{R}_2 E_+ \left(t - \frac{2L}{c}, x \right)$$

$$E_+(\omega,x) = \mathcal{T}_1 E_{in}(\omega,x) + \mathcal{R}_1 \mathcal{R}_2 e^{i\omega 2L/c} E_+(\omega,x)$$

where

$$E(\omega,x) = \int_{-\infty}^{+\infty} E(t,x) e^{-i\omega t} dt$$

The solution is straightforward, and we find

$$E_+\left(\omega, x\right) = \frac{\mathcal{T}_1}{1 - \mathcal{R}_1\mathcal{R}_2 e^{i\omega 2L/c}} E_{in}(\omega, x)$$

$$= \frac{\mathcal{T}_1}{\left[1 - \mathcal{R}_1\mathcal{R}_2 \cos(\omega\frac{2L}{c})\right] - i\mathcal{R}_1\mathcal{R}_2 \sin(\omega\frac{2L}{c})} E_{in}(\omega, x)$$

when we assume that mirrors do not introduce additional phase changes.
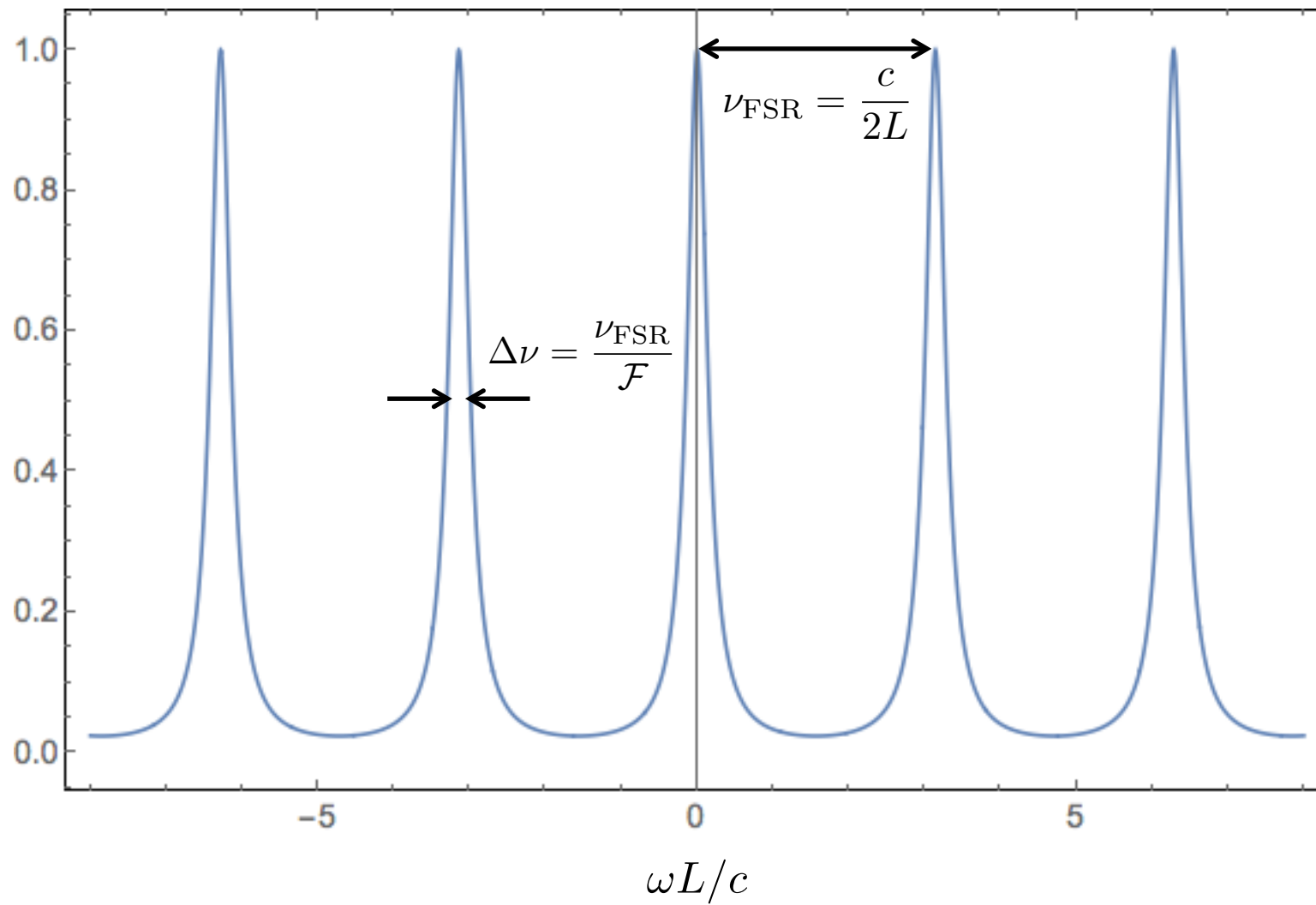
fppt.com

When we define the *finesse*

$$\mathcal{F} = \pi \frac{(\mathcal{R}_1 \mathcal{R}_2)^{1/4}}{1 - \sqrt{\mathcal{R}_1 \mathcal{R}_2}}$$
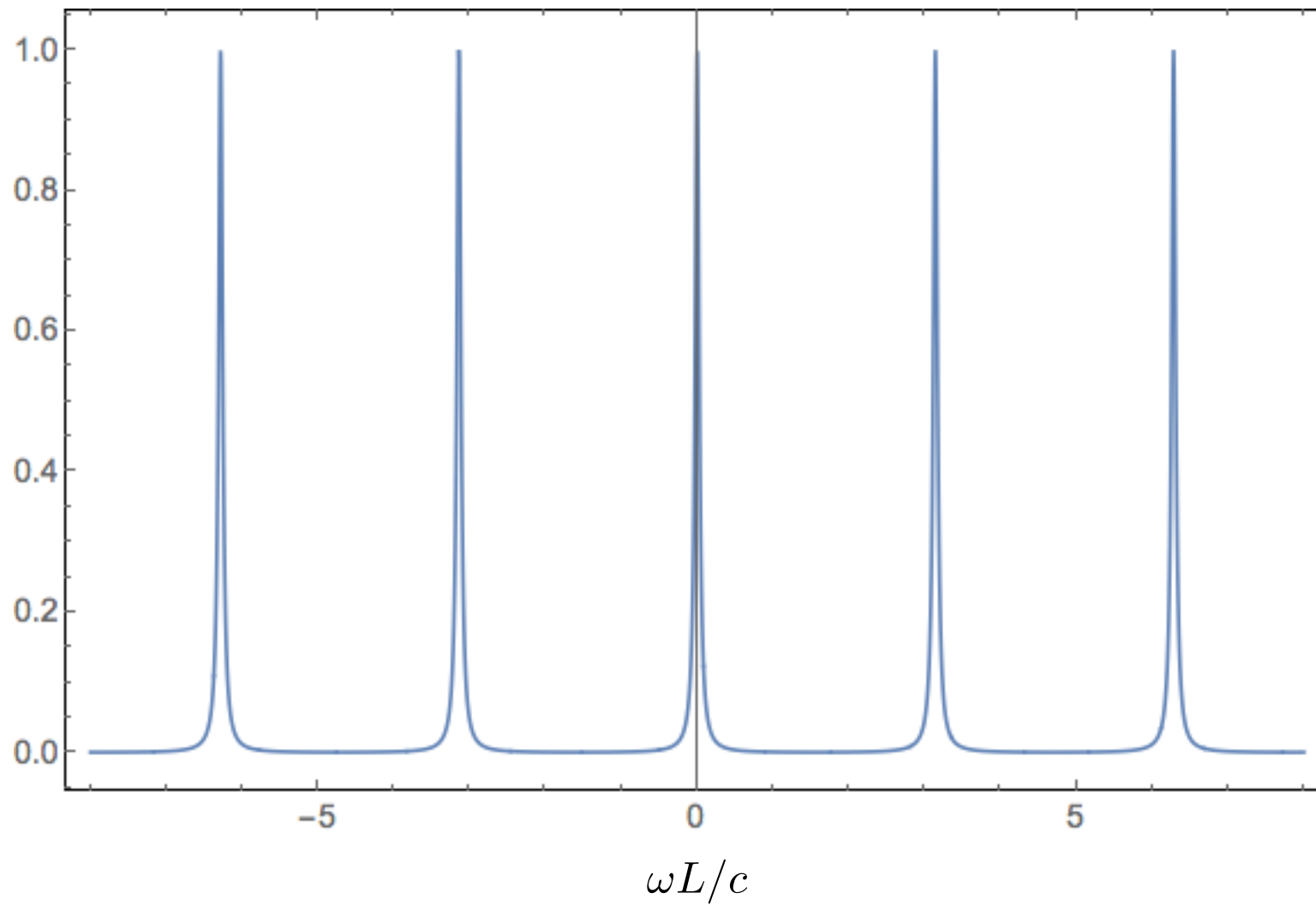
we can write

$$|E_+^{out}(\omega, x)|^2 = \frac{(1 - |\mathcal{R}_1|^2)(1 - |\mathcal{R}_2|^2)}{|1 - \mathcal{R}_1 \mathcal{R}_2|^2} \frac{1}{1 + \left(\frac{2\mathcal{F}}{\pi}\right)^2 \sin^2\left(\omega \frac{L}{c}\right)} |E_{in}(\omega, x)|^2$$

$$\frac{1}{1 + \left(\frac{2\mathcal{F}}{\pi}\right)^2 \sin^2\left(\omega \frac{L}{c}\right)} \quad \text{Airy curve}$$
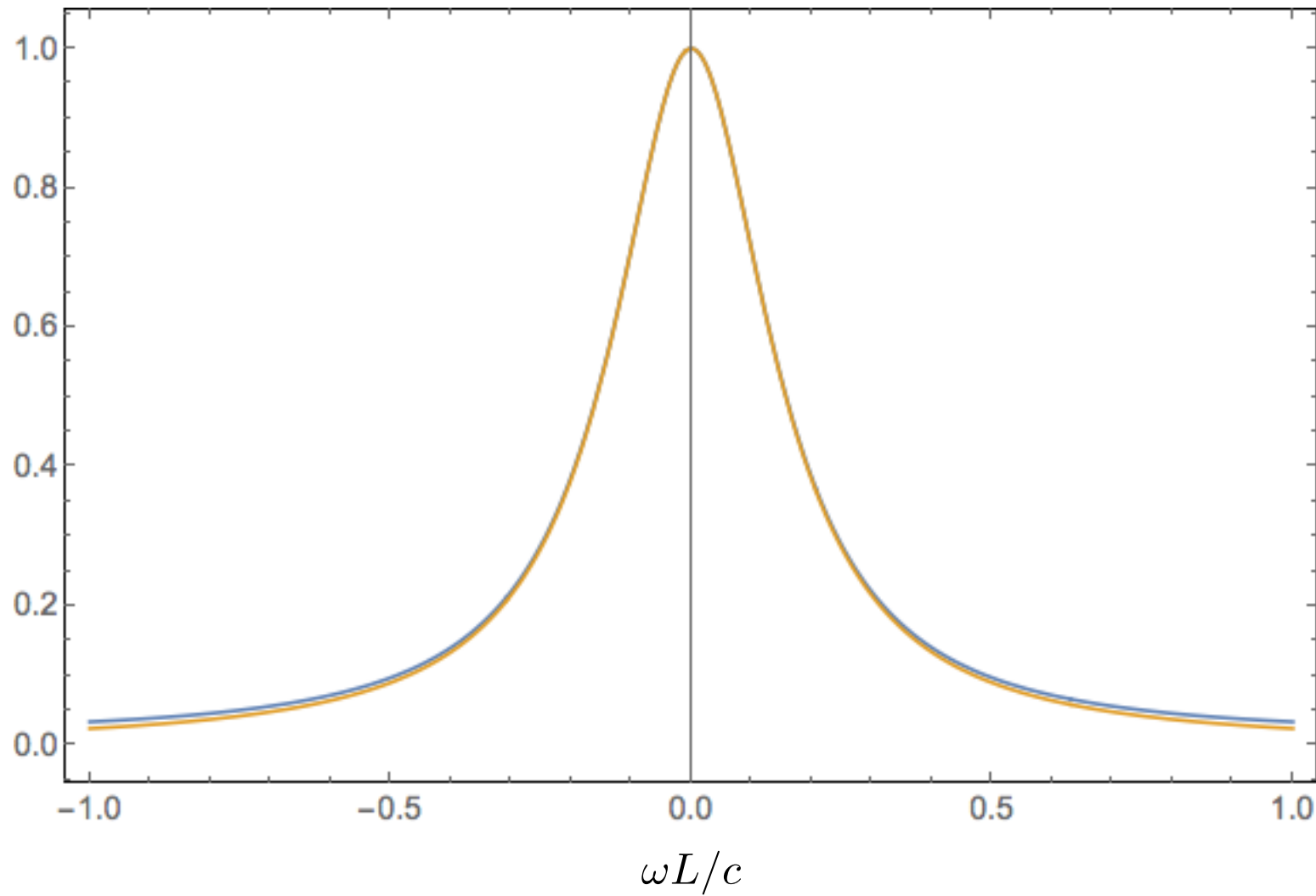
Airy curve $\mathcal{F} = 10$

$$\nu_{\mathrm{FSR}} = \frac{c}{2L}$$

$$\Delta\nu = \frac{\nu_{\mathrm{FSR}}}{\mathcal{F}}$$

$\omega L/c$

fppt.com

Airy curve $\mathcal{F} = 50$

$\omega L/c$

Airy curve $\mathcal{F} = 10$ and its Lorenzian approximant

Intensity loss per round trip in the resonator:

$$\exp\left(-2L\alpha\right) \approx |\mathcal{R}_1\mathcal{R}_2|^2$$

Relation with the finesse (for high finesse, i.e., high-reflectivity mirrors)

$$\mathcal{F} = \pi\frac{(\mathcal{R}_1\mathcal{R}_2)^{1/4}}{1 - \sqrt{\mathcal{R}_1\mathcal{R}_2}} \qquad \Longrightarrow \qquad \alpha = \frac{\pi}{L\mathcal{F}}$$

where α is the loss per unit length, therefore the loss per unit time is

$$\frac{1}{\tau} = c\alpha = \frac{\pi c}{L\mathcal{F}} = \frac{2\pi\nu_{\mathrm{FSR}}}{\mathcal{F}} \qquad \Longrightarrow \qquad \mathcal{F} = 2\pi\nu_{\mathrm{FSR}}\tau$$

The decay constant for the field amplitude is

$$\frac{\alpha}{2} = \frac{\pi}{2L\mathcal{F}}$$

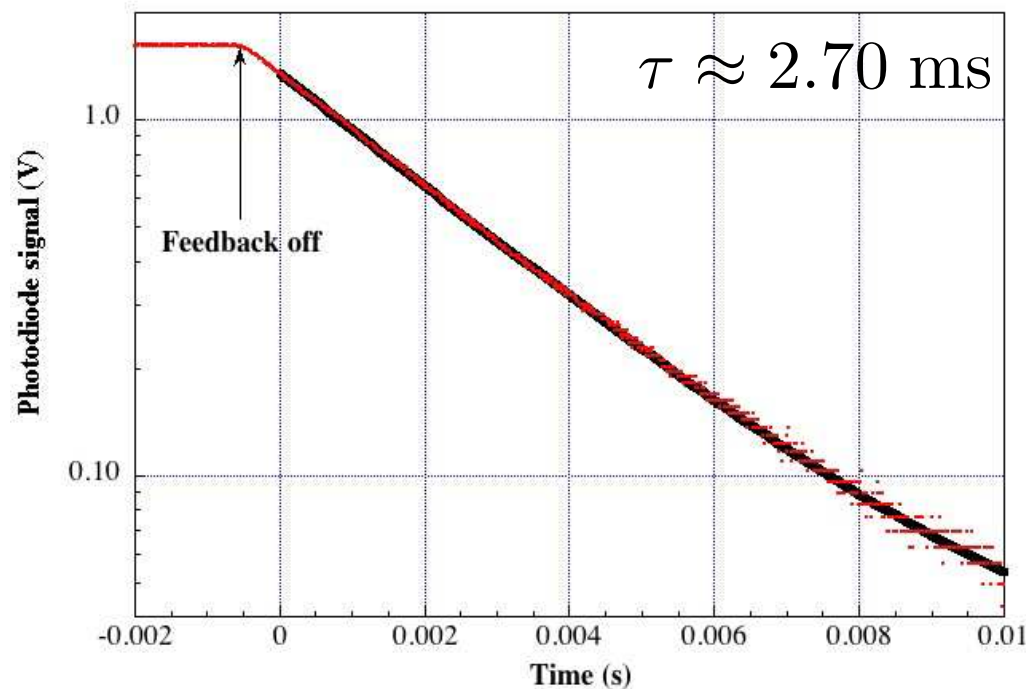therefore the mean effective length traveled by a wave inside the FP resonator is

$$\frac{2}{\alpha} = \frac{2L\mathcal{F}}{\pi}$$

so that the resonator achieves a path amplification factor

$$N = \frac{2\mathcal{F}}{\pi}$$

PVLAS @ Ferrara

$$\nu_{FSR} = \frac{c}{2L} \approx 4.55 \cdot 10^7 \text{ Hz}$$

$\tau \approx 2.70 \text{ ms}$

$\mathcal{F} \approx 770000$

$c\tau \approx 810 \text{ km}$

$N \approx 490000$

Fig. 3. Decay of the light transmitted from the cavity after switching off the laser frequency locking system. The decay is fitted with the exponential function $a + be^{-t/\tau_d}$, and gives for the decay time $\tau_d = 2.70 \pm 0.02$ ms.

Table 1. Summary of a few Fabry Perot cavities with longest decay time ever realized, together with the highest finesse for $\lambda = 1064$ nm and the highest finesse in absolute. The coherence length is defined as $\ell_c = c\tau_d$.

Cavity	Length (m)	τ_d (ms)	Finesse	$\delta\nu_c$ (Hz)	λ (nm)	$\ell_c/10^3$ m
VIRGO [18]	3000	0.16	50	1000	1064	48
PVLAS [19]	6.4	0.905	144 000	176	1064	272
LIGO [20]	4000	0.975	220	163	1064	293
BMV [10]	2.27	1.28	530 000	125	1064	384
This work	3.303	**2.7**	770 000	**59**	1064	**810**
This work	0.017	0.0143	789 000	11 100	1064	5.1
J. Millo et al.[21]	0.1		$\approx 800\,000$		1064	
G. Rempe et al.[12]	0.004	0.008	1 900 000	20 000	850	2.4

Detection of very small birefringences

A beam of linearly polarized light that goes through a birefringent crystal changes its polarization to elliptical
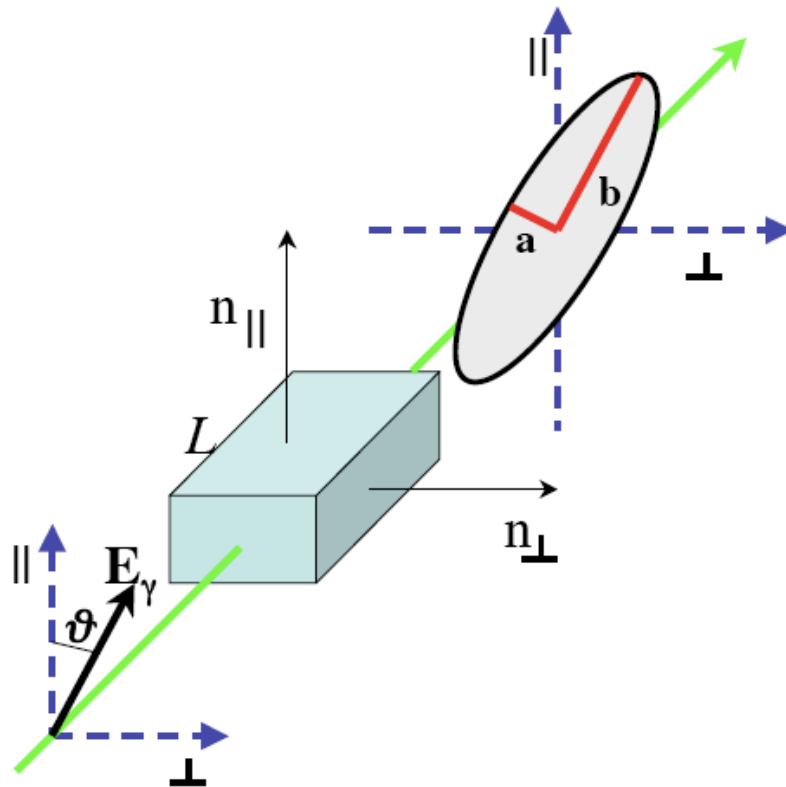
The *ellipticity* is defined as the ratio between minor and major axis of the ellipse, and it is related to the phase shift between the electric field components parallel to the crystal axes

$$\psi = \frac{a}{b} = \frac{\pi L}{\lambda} \Delta n \sin 2\vartheta$$

Since the expected QED birefringence with a 2.5 T magnetic field is

$$\Delta n|_{B=2.5 \text{ T}} \approx 2.5 \ 10^{-23}$$

with a magnetic field region L = 2 m, a NdYAG infrared laser (wavelength = 1032 nm), and a finesse 770000

$$\psi \approx 7 \ 10^{-11}$$

**Thus, measuring the QED effect is an extremely challenging task, even with such a high-finesse resonator.**

To detect physical effects we must modulate them (or turn them ON and OFF). Here we do it by rotating the magnetic field
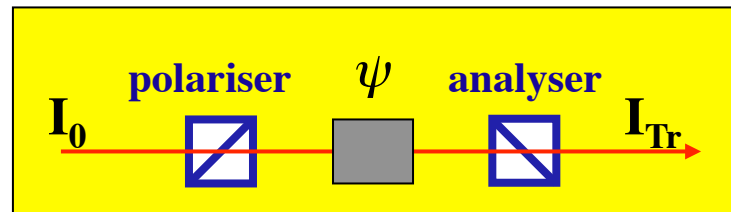
$$I_{tr} = I_0 \left[\sigma^2 + \psi^2 \right]$$

extinction

ellipticity

In this simple scheme the transmitted intensity is proportional to the *square* of the ellipticity, and modulation produces an exceedingly small effect !!! (of the order of 10^{-21} in our case)
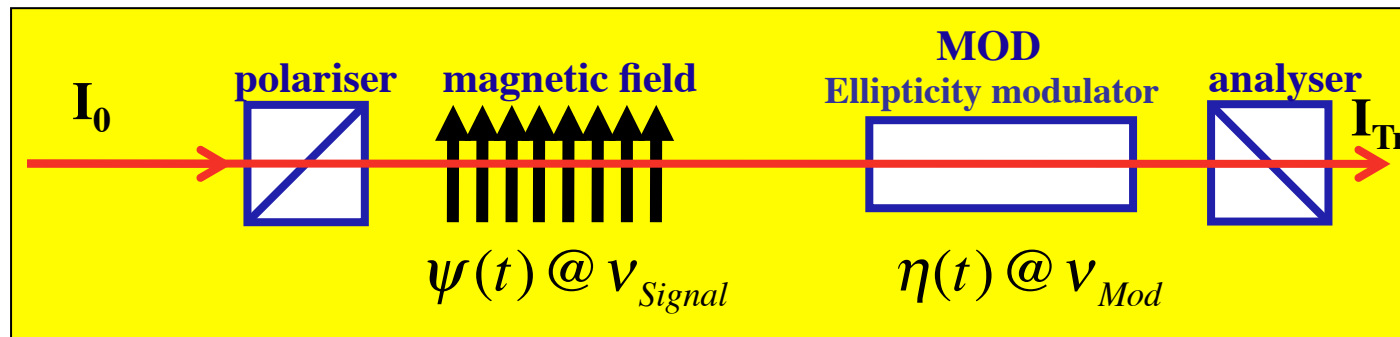
$$I_{Tr} = I_0\left[\sigma^2 + \left(\psi(t) + \eta(t)\right)^2\right] = I_0\left[\sigma^2 + \left(\psi(t)^2 + \eta(t)^2 + 2\psi(t)\eta(t)\right)\right]$$

Using an ellipticity modulator the transmitted intensity is proportional to the the ellipticity, and – although difficult – a measurement becomes possible.

The ellipticity modulator also minimizes the annoying 1/f noise.

Frequency	Fourier component	Intensity/I_{out}	Phase
dc	I_{dc}	$\sigma^2 + \alpha_{\text{dc}}^2 + \eta_0^2/2$	$-$
ν_{Mod}	$I_{\nu_{\text{Mod}}}$	$2\alpha_{\text{dc}}\eta_0$	θ_{Mod}
$\nu_{\text{Mod}} \pm 2\nu_{\text{Mag}}$	$I_{\nu_{\text{Mod}}\pm 2\nu_{\text{Mag}}}$	$\eta_0 \dfrac{2\mathcal{F}}{\pi}\psi$	$\theta_{\text{Mod}} \pm 2\vartheta_{\text{Mag}}$
$2\nu_{\text{Mod}}$	$I_{2\nu_{\text{Mod}}}$	$\eta_0^2/2$	$2\theta_{\text{Mod}}$
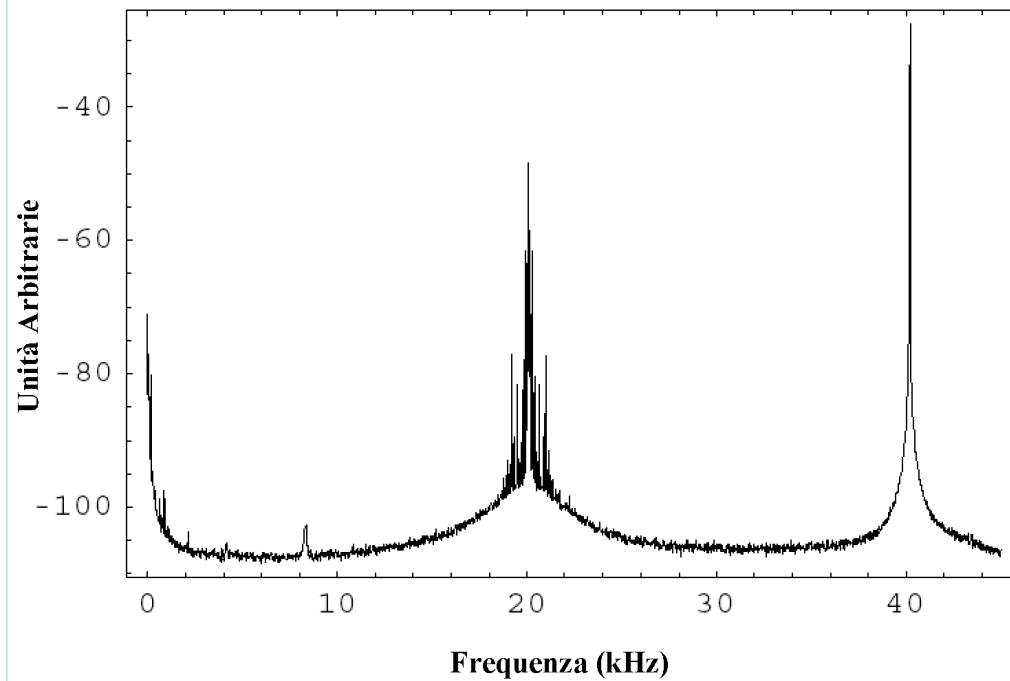
$$\Psi = \frac{1}{2}\left(\frac{I_{\nu_{\text{Mod}}+2\nu_{\text{Mag}}}}{\sqrt{2I_{\text{out}}I_{2\nu_{\text{Mod}}}}} + \frac{I_{\nu_{\text{Mod}}-2\nu_{\text{Mag}}}}{\sqrt{2I_{\text{out}}I_{2\nu_{\text{Mod}}}}} \right)$$

Noise issues and experimental sensitivity

$$s_{\text{shot}} = \sqrt{\frac{2e}{I_{\text{out}}q}\left(\frac{\sigma^2 + \eta_0^2/2}{\eta_0^2}\right)}$$

Shot noise: can be reduced by increasing power and reducing extinction

For 10 mW intensity $s_{\text{shot}} = 7\ 10^{-9}\ 1/\sqrt{\text{Hz}}$

$$s_{\text{dark}} = \frac{V_{\text{dark}}}{G}\frac{1}{I_{\text{out}}\,q\,\eta_0}$$

Photodetector noise: can be reduced by increasing power, and with better detector

$$s_J = \sqrt{\frac{4k_BT}{G}}\frac{1}{I_{\text{out}}\,q\,\eta_0}$$

Johnson noise: can be reduced by increasing power

$$s_{\text{RIN}} = \text{RIN}(\nu_{\text{Mod}})\frac{\sqrt{(\sigma^2 + \eta_0^2/2)^2 + (\eta_0^2/2)^2}}{\eta_0}$$

Light intensity noise: can be reduced by reducing extinction, stabilizing power, increasing modulator frequency

+ all other uncontrolled sources of **time variable birefringences** *a(t)*

1/f noise: can be reduced by increasing the modulator frequency

Test and calibration can be carried out using the Cotton-Mouton effect in gases

A gas at a pressure p in presence of a transverse magnetic field B becomes birefringent.

$$\Delta n = n_{\parallel} - n_{\perp} = \Delta n_u \left(\frac{B[\text{T}]}{1\text{T}} \right)^2 \left(\frac{P}{P_{atm}} \right)$$

Total ellipticity

$$\psi_{gas} = N\pi \frac{L}{\lambda} \Delta n_u B^2 p \sin 2\vartheta$$

Gas	Δn_u (T ~ 293 K)
N_2	- $(2.47 \pm 0.04) \times 10^{-13}$
O_2	- $(2.52 \pm 0.04) \times 10^{-12}$
CO	- $(1.83 \pm 0.05) \times 10^{-13}$

Moreover, to check for spurious effects in a QED run, the residual gas must be analysed:

e.g., $p(O_2) < 10^{-8}$ mbar
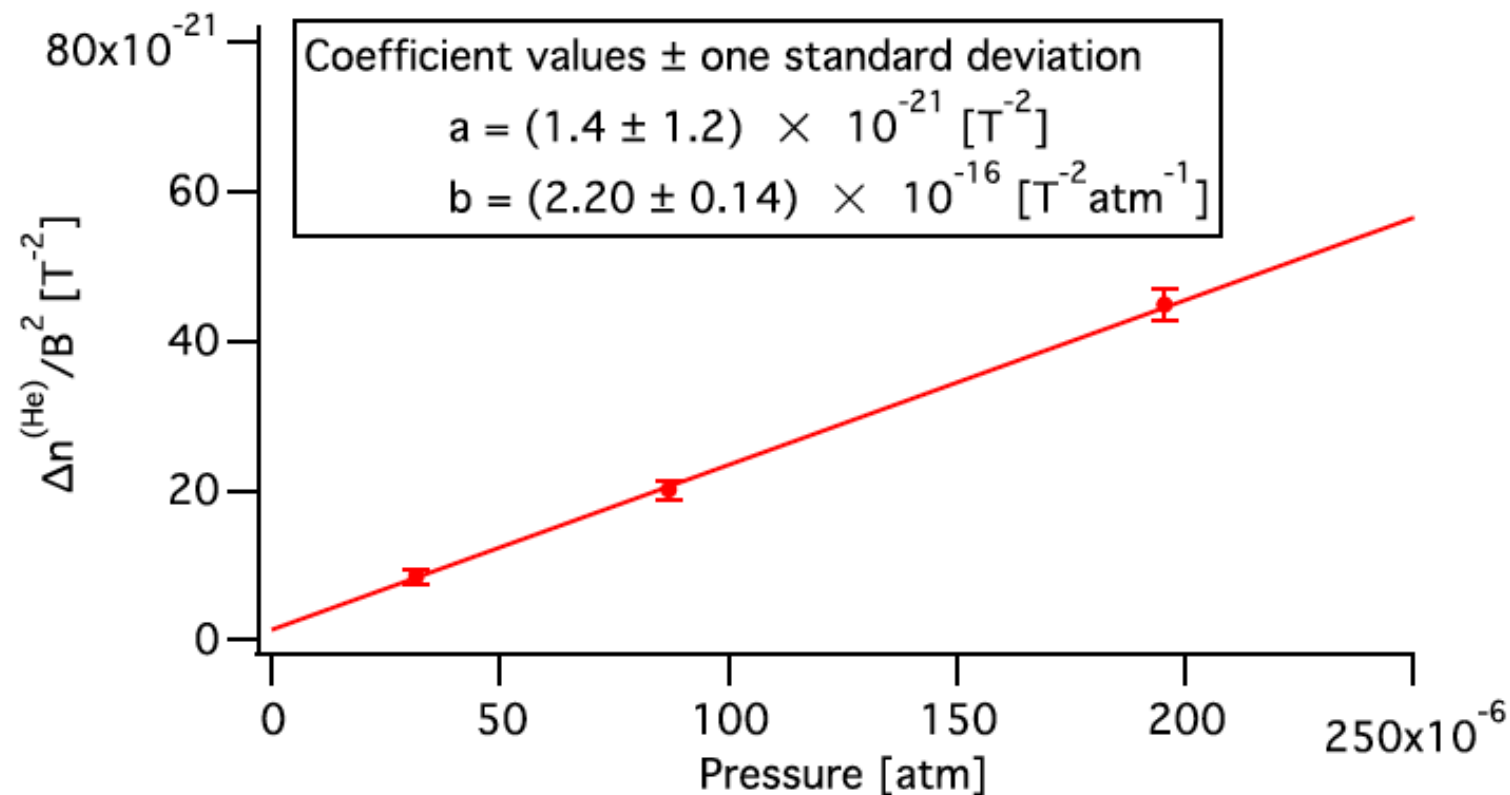
FIG. 3 (color online). Measured $\Delta n^{(\mathrm{He})}/B^2$ as a function of pressure P. The error bars correspond to a 1σ statistical error. The data are fitted with a linear function $a + bP$.
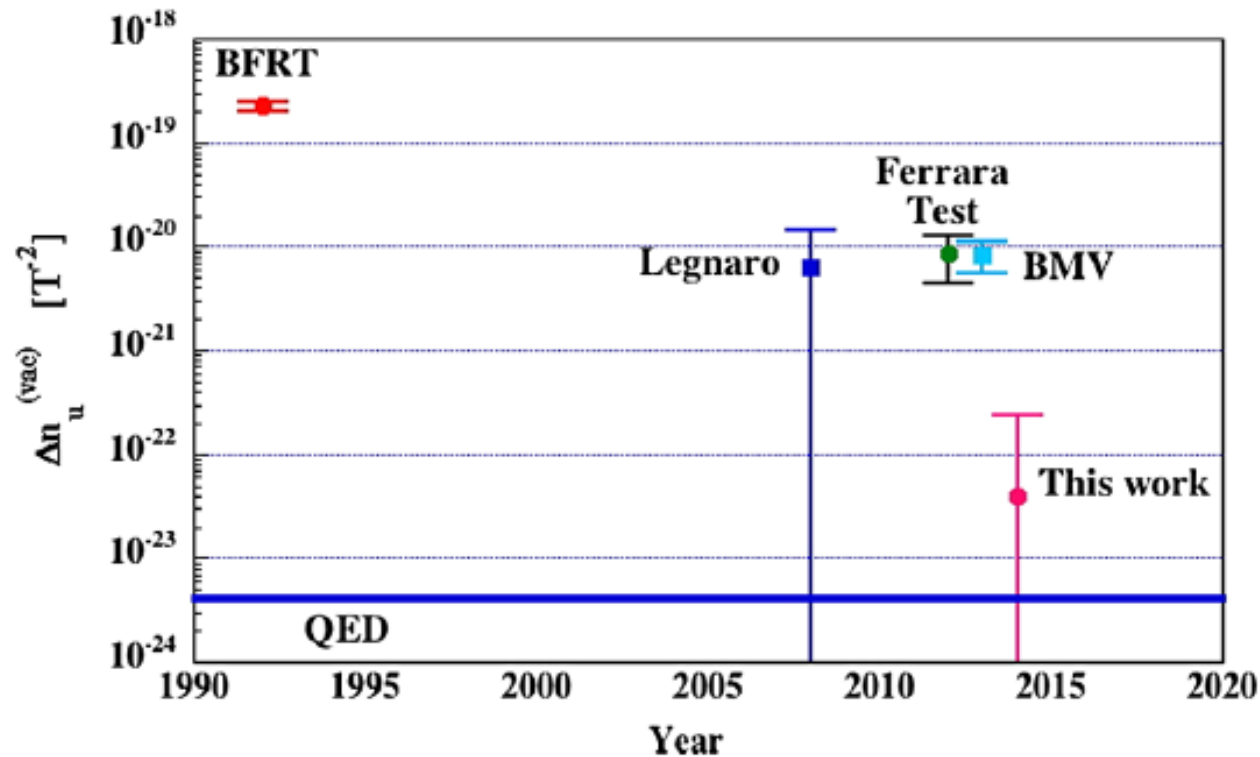
Where are we now?

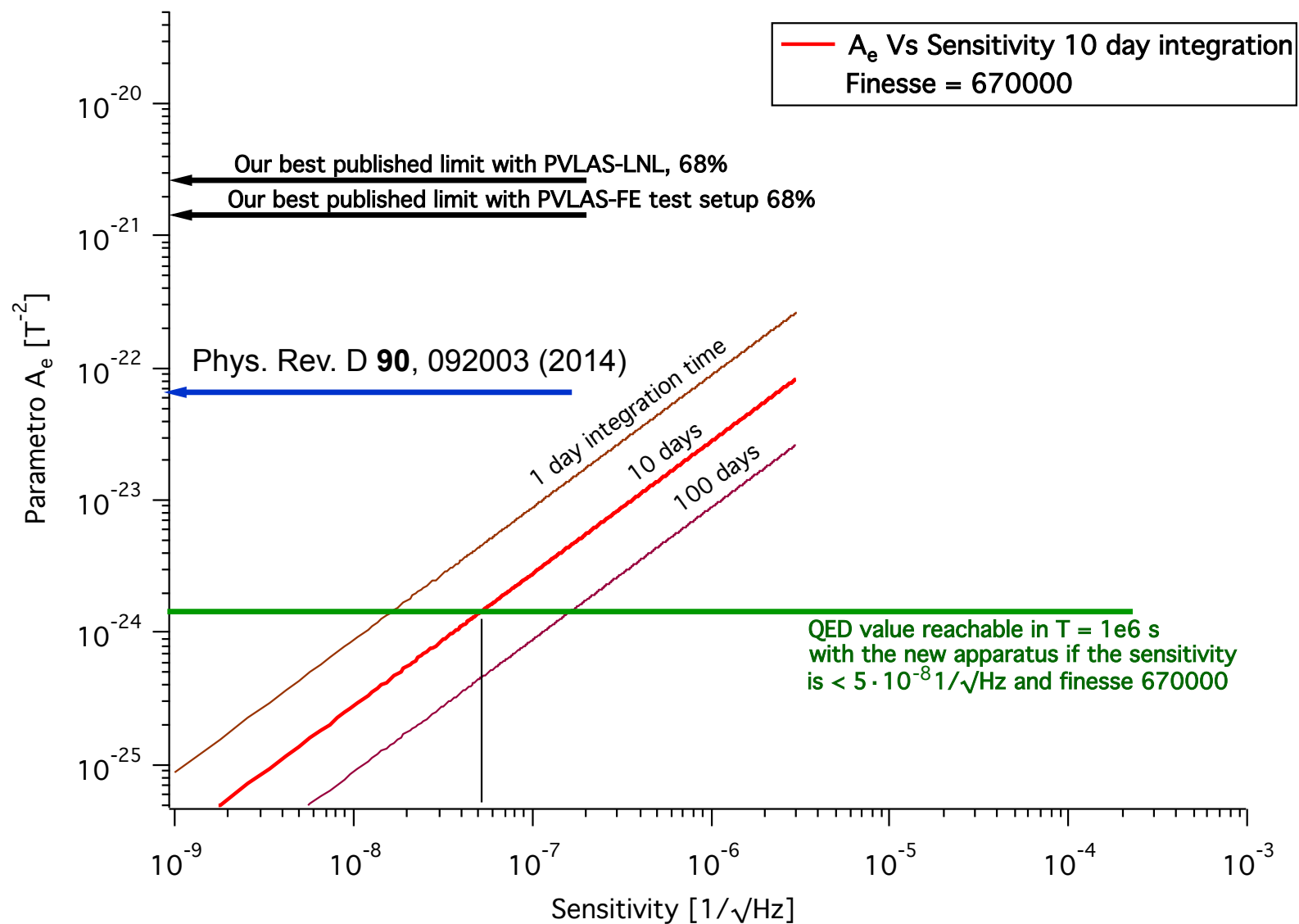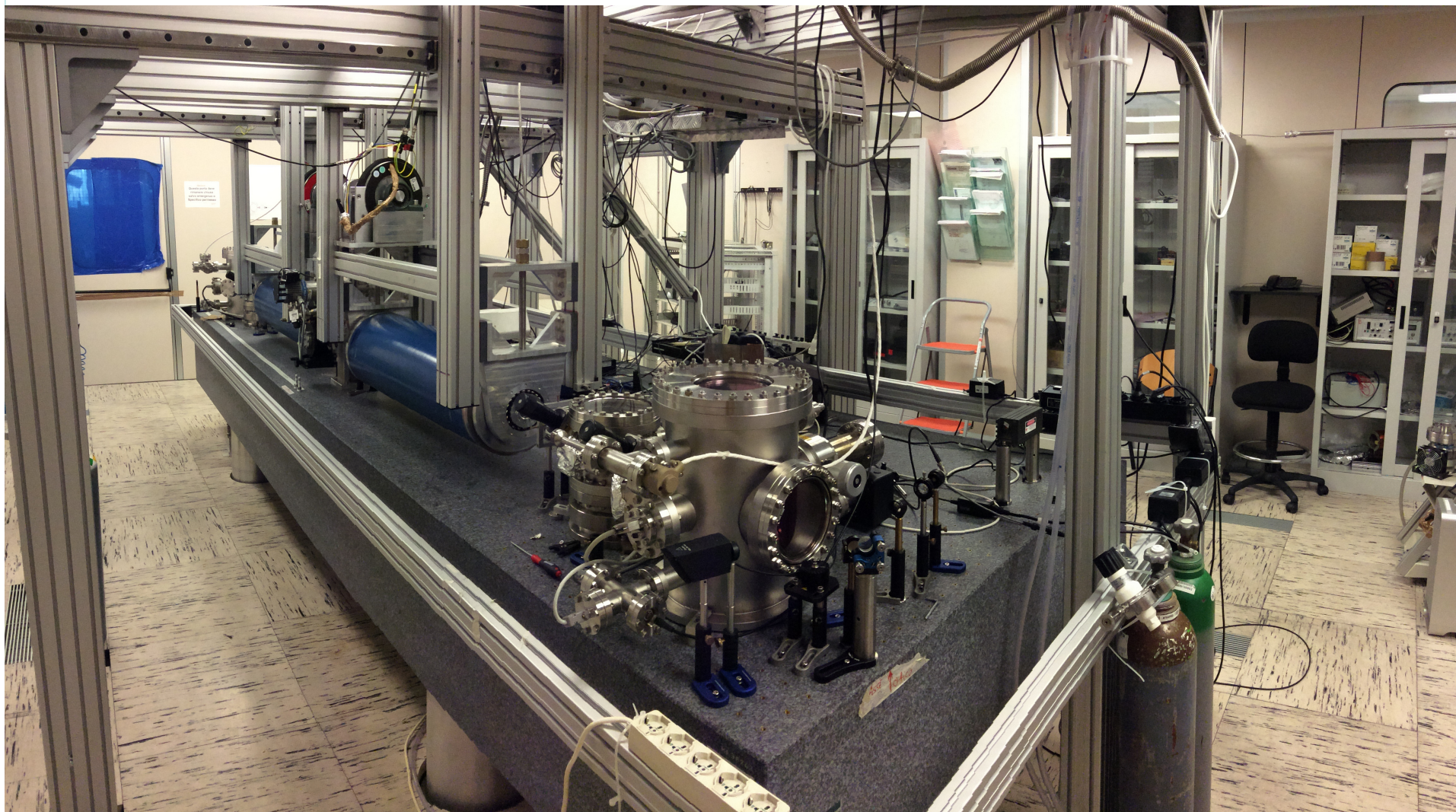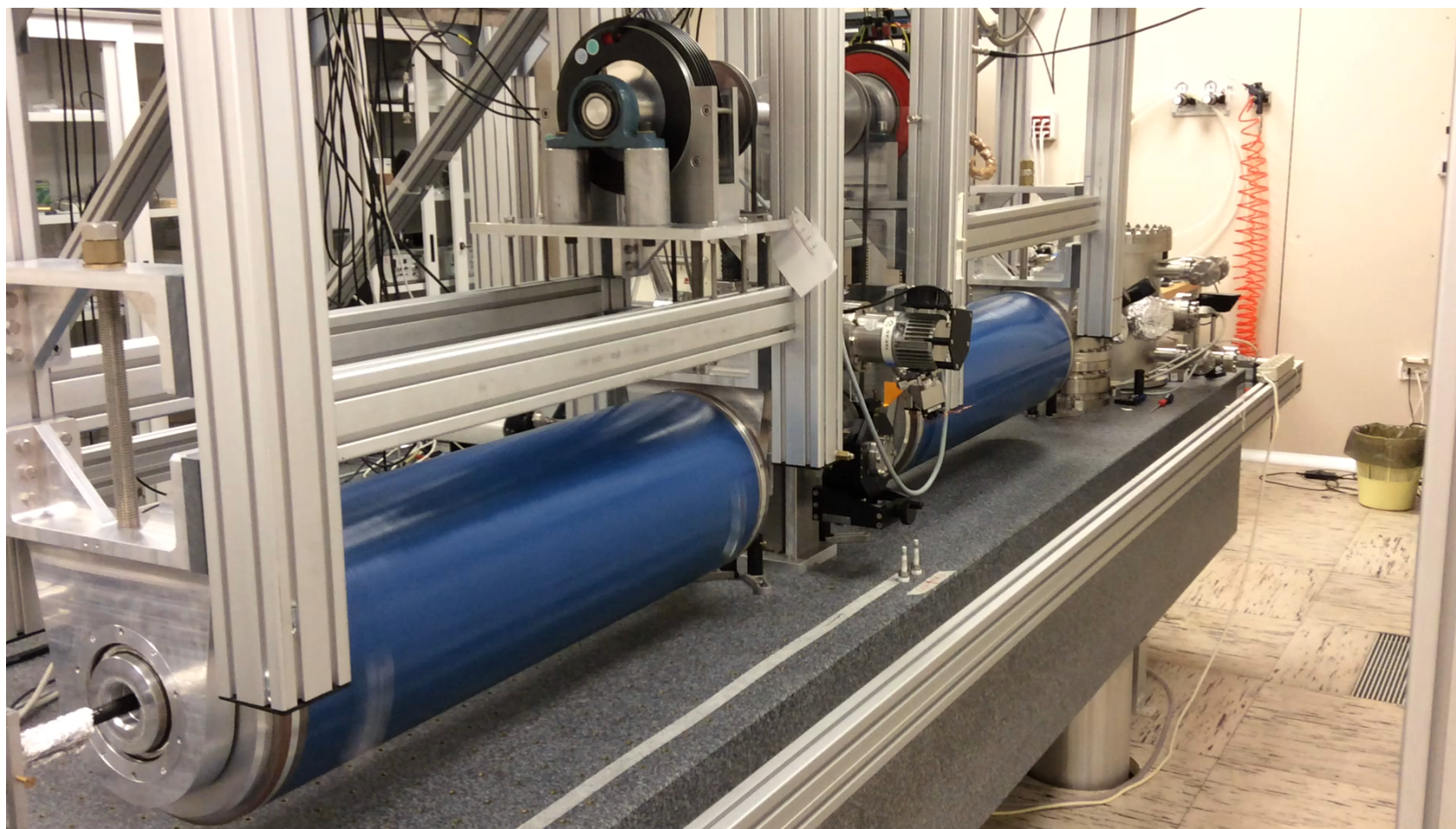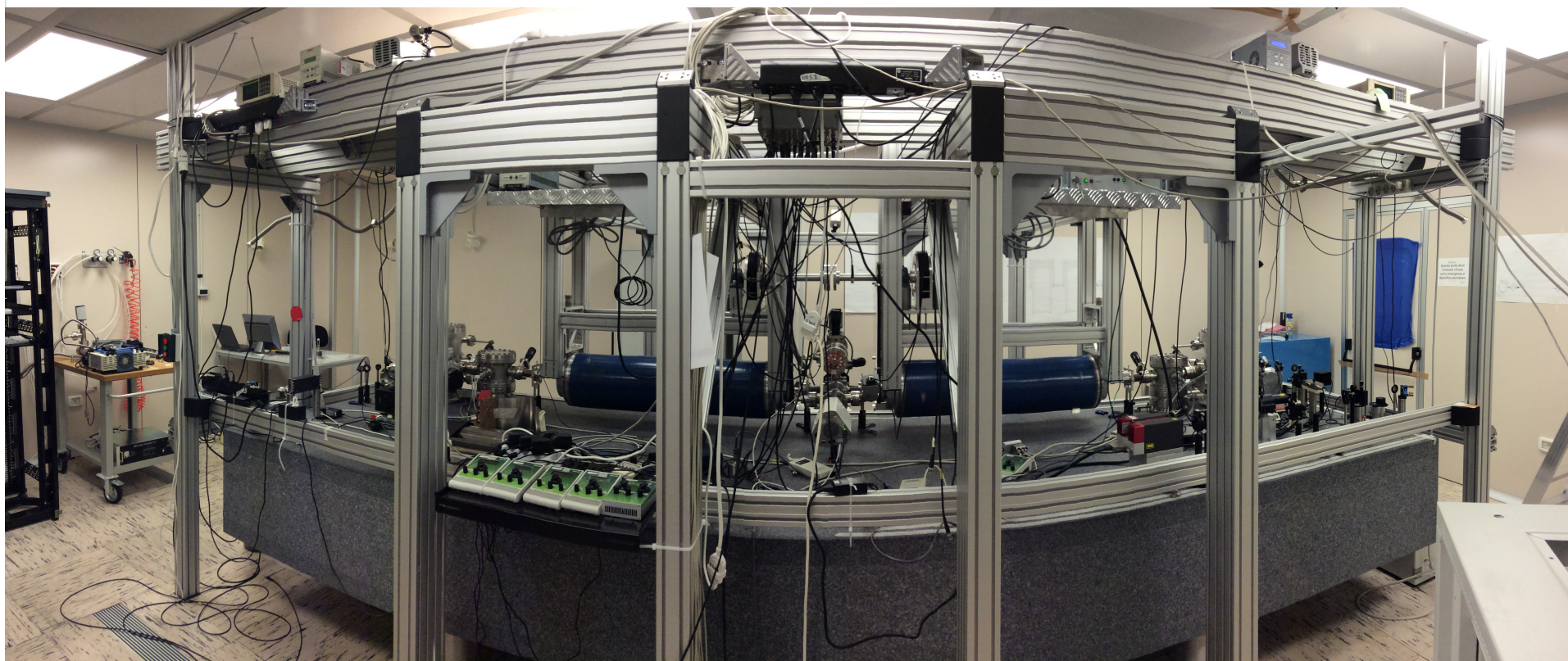FIG. 5 (color online). Comparison of published results for $\Delta n_u^{(vac)}$ of ellipsometric experiments (BFRT = [7], Legnaro = [15], Ferrara test = [16], BMV = [25]). The error bars correspond to a 1σ C.L.

Edoardo Milotti – University of Trieste and I.N.F.N.-Sezione di Trieste

59

Edoardo Milotti – University of Trieste and I.N.F.N.-Sezione di Trieste

61

Why try to confirm the QED prediction? How could the QED vacuum be any different?

The class of effective Lagrangians that satisfy the basic QFT constraints

- Lorentz- and gauge-invariance
- locality, i.e., only first order derivatives of the fields are admissible,
- parity invariance

up to fourth order in the fields, the Lagrangian can be parameterized as follows (parameterized post-Maxwellian Lagrangian)

$$\mathcal{L} = -\mathcal{F} + c_1 \mathcal{F}^2 + c_2 \mathcal{G}^2$$

where $\quad \mathcal{F} = \dfrac{1}{4} F_{\mu\nu} F^{\mu\nu} = \dfrac{1}{2}(\mathbf{E}^2 - \mathbf{B}^2); \quad \mathcal{G} = \dfrac{1}{4} F_{\mu\nu} \tilde{F}^{\mu\nu} = \mathbf{E} \cdot \mathbf{B}$

and $\quad c_1^{(QED)} = \dfrac{8\alpha^2}{45 m_e^4}; \quad c_2^{(QED)} = \dfrac{14\alpha^2}{45 m_e^4}$

A notable member of this class of Lagrangians is the Born-Infeld Lagrangian (originally introduced to solve the divergence of electron EM self-energy)

$$\mathcal{L}_{BI} = b^2 \left(\sqrt{-\det \eta_{\mu\nu}} - \sqrt{-\det \eta_{\mu\nu} + F_{\mu\nu}/b} \right)$$

$$= b^2 \left(1 - \sqrt{1 + 2\mathcal{F}/b^2 - \mathcal{G}^2/b^4} \right)$$

$$\approx -\mathcal{F} + \frac{1}{2b^2}\mathcal{F}^2 + \frac{1}{2b^2}\mathcal{G}^2$$

$$= -\frac{1}{2}(\mathbf{E}^2 - \mathbf{B}^2) + \frac{1}{8b^2}(\mathbf{E}^2 - \mathbf{B}^2)^2 + \frac{1}{2b^2}(\mathbf{E} \cdot \mathbf{B}^2)^2$$

then $\quad c_1^{(BI)} = c_2^{(BI)} = 1/2b^2$

The BI Lagrangian surfaces in low-energy extrapolations of string theories.

An important and unique feature of the BI Lagrangian is that magnetized vacuum does not become birefringent.

Enter the strong CP problem

As Roberto Peccei nicely put it (Nucl. Phys. B72 (1999) 3)

"The strong CP problem is intimately connected with the failure of symmetries to survive quantum effects. ... "

The anomaly that leads to the strong CP problem can be cured with the introduction of a new pseudoscalar field, the axion, and this induces the appearance of a new term in the Lagrangian, which corresponds to the axion-photon interaction

The axion field couples to gluons and quarks, and thus it also couples to photons, via the anomaly diagram with a quark loop
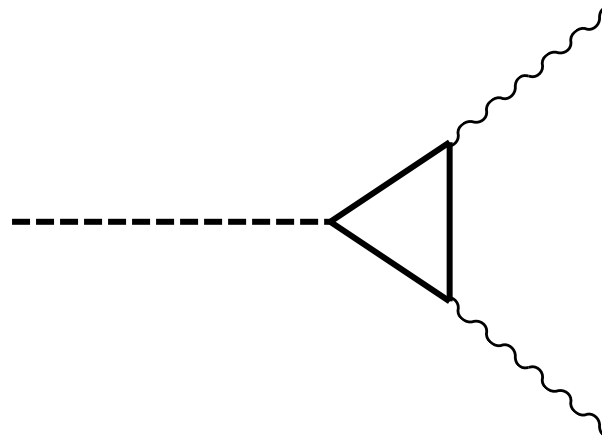
and therefore it is – in a way – related to the neutral pion.

This also means that the EM Lagrangian acquires a new, effective term, which is not P-invariant and it changes the phenomenology of photon-photon interactions

$$\frac{g}{4} a F^{\mu\nu} \tilde{F}_{\mu\nu} = -ga\mathbf{E} \cdot \mathbf{B}$$

Axion propagation in strong background static fields

As an offshoot of the QCD anomaly we obtain the effective axion-photon interaction Lagrangian

$$\mathcal{L}_P = \frac{1}{4M} a F_{\mu\nu} \tilde{F}^{\mu\nu} = -\frac{a}{M} \mathbf{E} \cdot \mathbf{B}$$

and when we split the EM tensor in photon + bkg field

$$F_{\mu\nu} = F_{\mu\nu}^{(\text{ext})} + \partial_\mu A_\nu - \partial_\nu A_\mu$$

and we keep only the terms that are linear in the fields, we find a set of coupled differential equations

$$0 = \Box \mathbf{A} + \frac{1}{M}\frac{\partial a}{\partial t}\mathbf{B}$$

$$0 = -\frac{1}{M}\mathbf{B} \cdot \frac{\partial \mathbf{A}}{\partial t} + (\Box + m^2)a$$

clearly only the component of the probe field that is parallel to the external magnetic field is affected by the axion field.

On the whole the axion changes light propagation in two different ways:

- the parallel field component is delayed with respect to the perpendicular field component and this produces a phase shift between the fields and therefore ellipticity

- when the axion has a very small mass it can be nearly on mass shell and propagate as such outside the resonator: this produces an energy loss in the parallel field component and therefore dichroism

Scalar particles

In addition to pseudoscalar axion-like particles we can consider hypothetical scalar particles as in the MPZ paper

$$\mathcal{L}_S = -\frac{1}{4M_S}\sigma F_{\mu\nu}F^{\mu\nu} = \frac{\sigma}{2M_S}(\mathbf{E}^2 - \mathbf{B}^2)$$

Both pseudoscalar and scalar particles have been considered as viable dark matter candidates.

It is easy to see that with scalars there is an inversion of the roles of the parallel and perpendicular field components.

The full discussion of the coupled equations of motion with a pseudoscalar / scalar is given in

- Maiani, Petronzio & Zavattini, Phys. Lett. B 175 (1986) 359
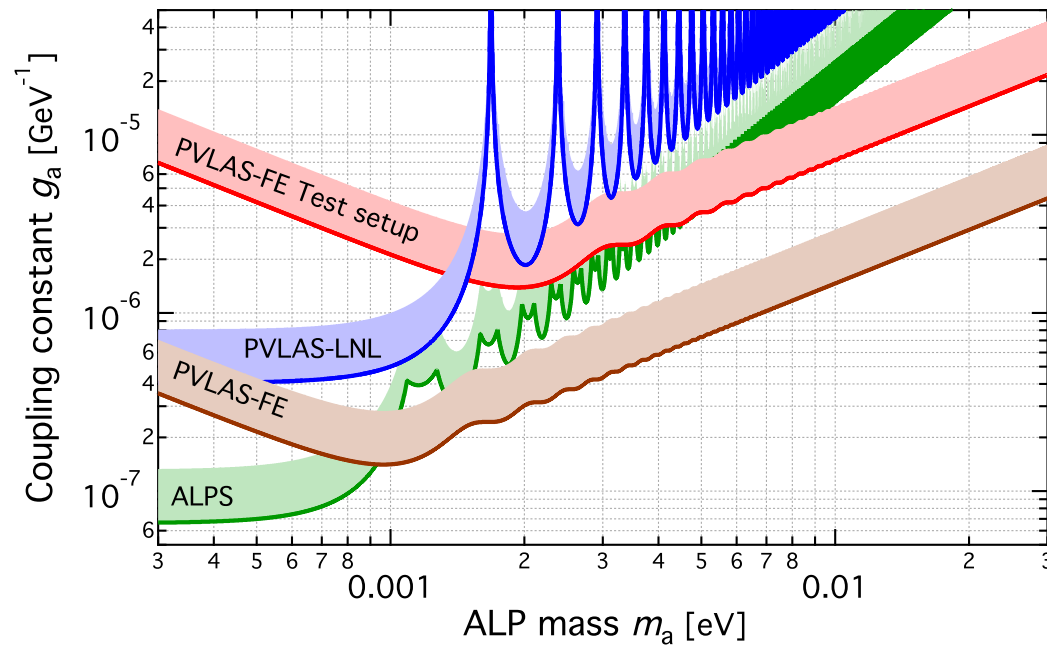
- Gasperini, Phys. Rev. Lett. 59 (1987) 396

FIG. 6 (color online). Updated 95% C.L. exclusion plot for axion-like particles. In green, limits from the ALPS Collaboration [40] are shown; in blue, limits from dichroism measurements performed by PVLAS at LNL [8]; in red, limits from the ellipticity measurements performed with the test setup in Ferrara [16]. The results described in this paper lead to a new bound, shown in brown. Preliminary results from the OSQAR Collaboration can be found in Ref. [41]. They are very similar to the results from ALPS.

Axions are often prized as important components of dark matter, and for their role in superstring theory and more.

At least in the context of experiments such as PVLAs, the concept of axions is to be valued for the insight that it provides into the nature of field theory.

An example of the deeper theoretical understanding that could be associated to the inner nature of axions comes not from HEP, but from down-to-earth solid state science.

The applications of axion electrodynamics studied by F. Wilczek in 1987 (PRL 58 (1987) 1799), popped up rather unexpectedly in the behavior of topological insulators.
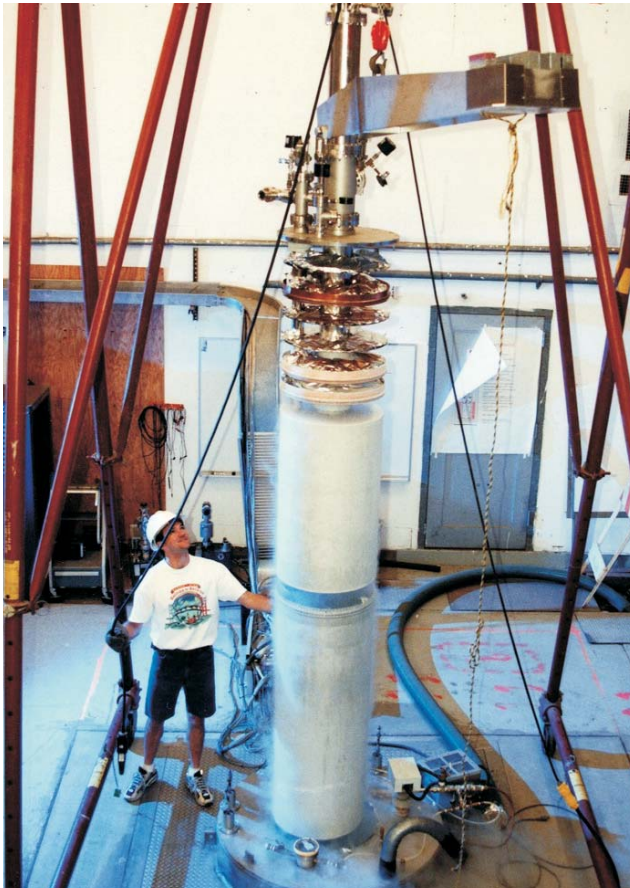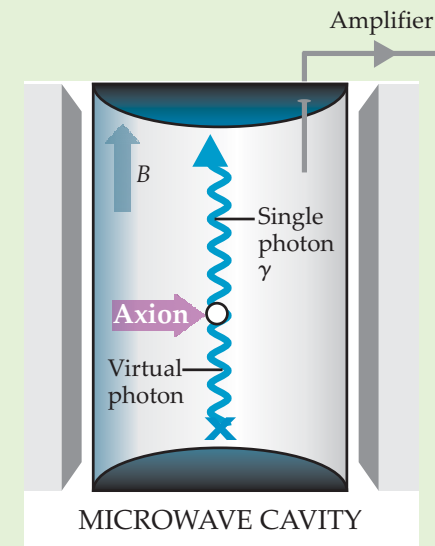
ADMX experiment

Figure 1. The Axion Dark Matter Experiment at Lawrence Livermore National Laboratory is designed to detect an axion by its decay into a single, real microwave photon in the presence of a magnetic field *B*. The experiment consists of three basic components: a powerful 8-tesla superconducting magnet, a high-*Q* and tunable cavity, and an ultrasensitive microwave amplifier as the front end of a radio receiver. The experimental tower is shown here being withdrawn from the magnet and cryostat, which extends 4 meters below floor level. The exposed disks are thermal shields to insulate the cavity and detector electronics held at 1.5 K. The challenge is to detect any slight excess in microwave photons in a narrow peak above thermal and electronic noise during a search.

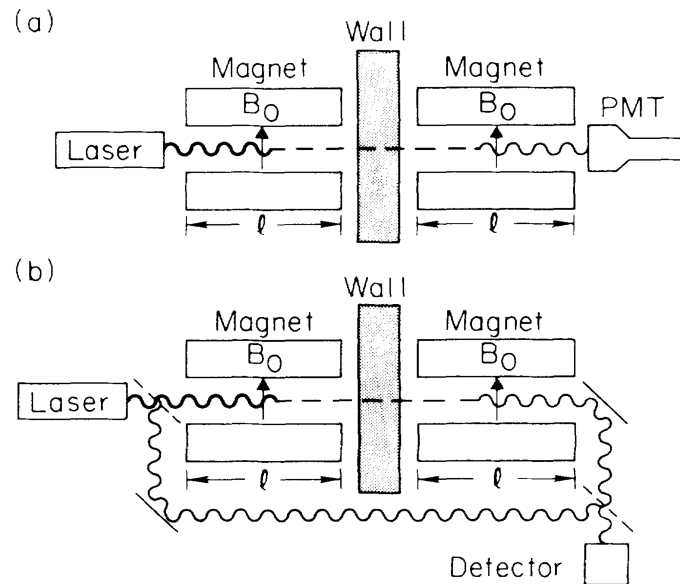## "Light shining through walls"

FIG. 1. Experimental setups. (a) Photons from a laser are shone into the bore of a dipole magnet. There the real laser photons interact with the virtual photons from the magnetic fields, producing pseudoscalars. The weakly interacting pseudoscalars penetrate the wall and then convert in the second magnet. The resulting photon is detected in the phototube (PMT). (b) A similar experiment, except that interference is used to increase the signal-to-noise ratio.

from Van Bibber et al, PRL **59** (1987) 759

In the 1980's, a straightforward setup to detect light pseudoscalars using the scheme called "light shining through a wall" was proposed.

This scheme has spawned several experiments. To date no signal has ever been detected.

fppt.com

Photon-photons scattering experiments in different regimes

peak cross section, ≈1.6 μbarn at
$$\hbar\omega \approx 1.5 m_e c^2$$

E_{CM} (MeV)
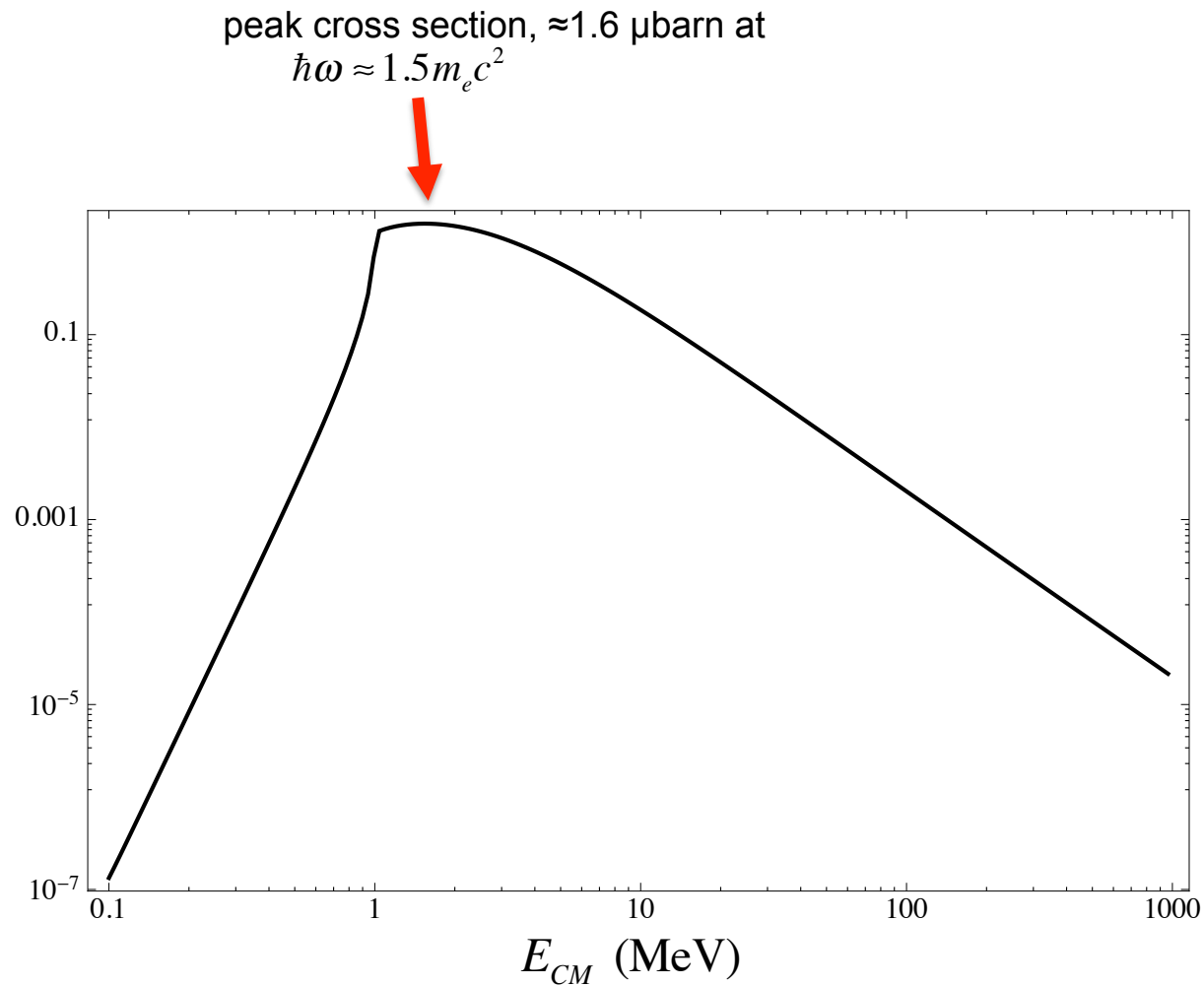
STAR = Southern Europe Thomson source for Applied Research

UniCal Campus

# A Photon-Photon Scattering Machine based on twin Photo-Injectors and Compton Sources

- Mono-chromatic High Brilliance micron-spot psec Gamma Ray beams are needed for pursuing Photon-Photon scattering experiments at high luminosity

- Similar to those generated by Compton (back-scattering) Sources for Nuclear Physics/Photonics

- (mini) Colliders similar to γ−γ colliders, but at low energy (in the 0.5-2 MeV range)

- *Best option: twin system of X-band 200 MeV photo-injectors with Compton converters and amplified J-class ps lasers (ELI-NP-GBS/ STAR) – single bunch no laser re-circulation*
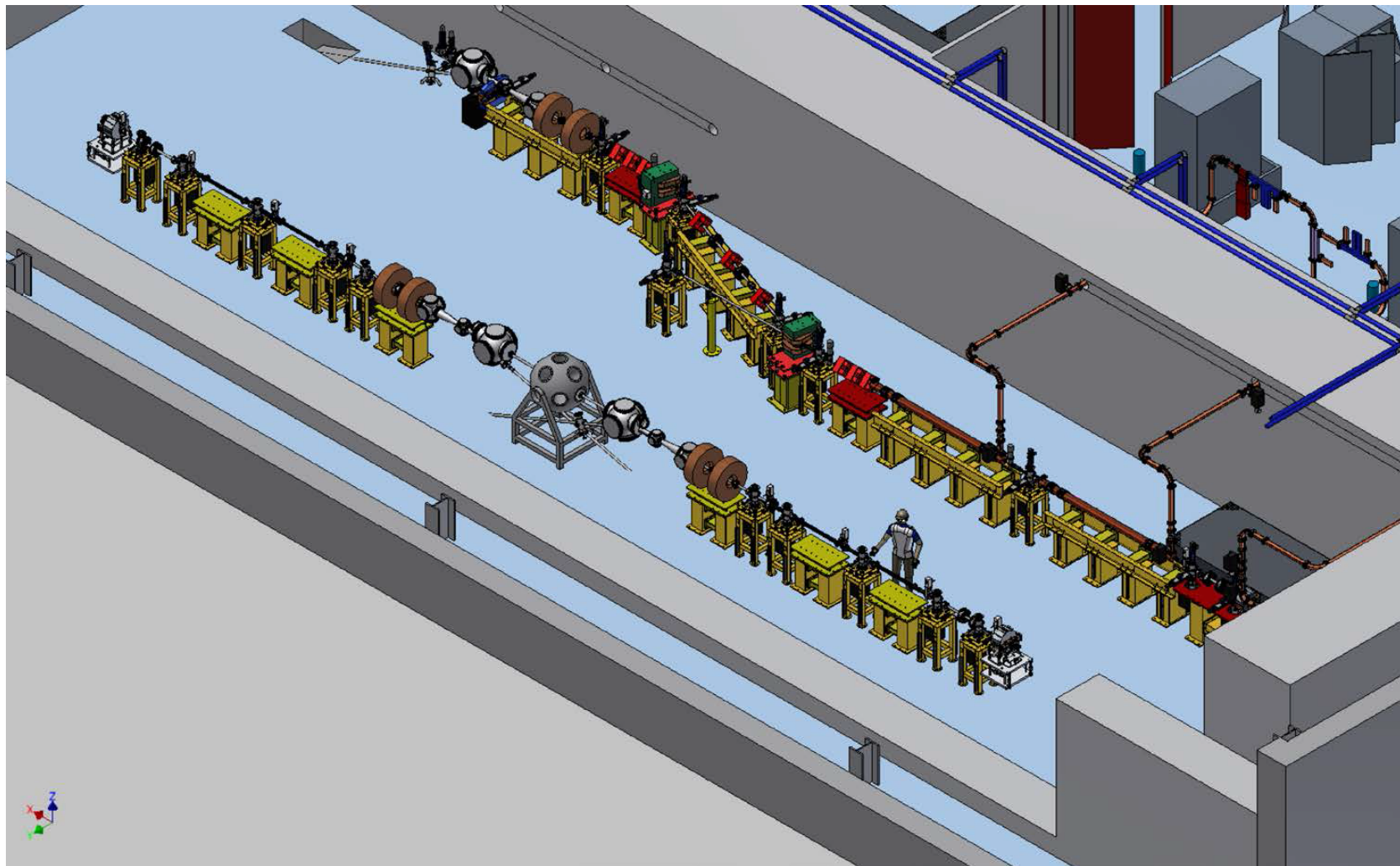
fppt.com

Strawman Design of Photon-Photon Scattering machine
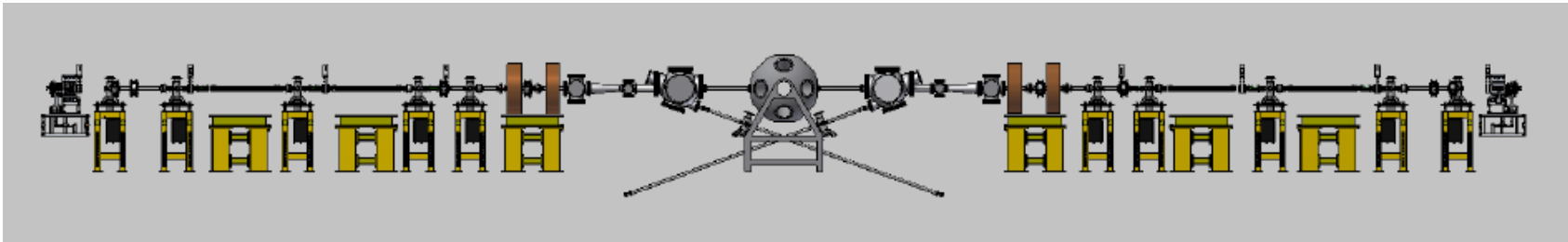
Colliding 2 gamma-ray 0.5 MeV beams, carrying 10^9 photons per pulse at 100 Hz rep rate, with focal spot size at the collision point of about 2 µm, we achieve:

- $L_{SC} = 2 \cdot 10^{26}$
- cross section = 1 µbarn, events/s=2.10^{-4}, events/day=18
- 1 nanobarn^{-1} accumulated after 3.2 months of 5/24 machine running
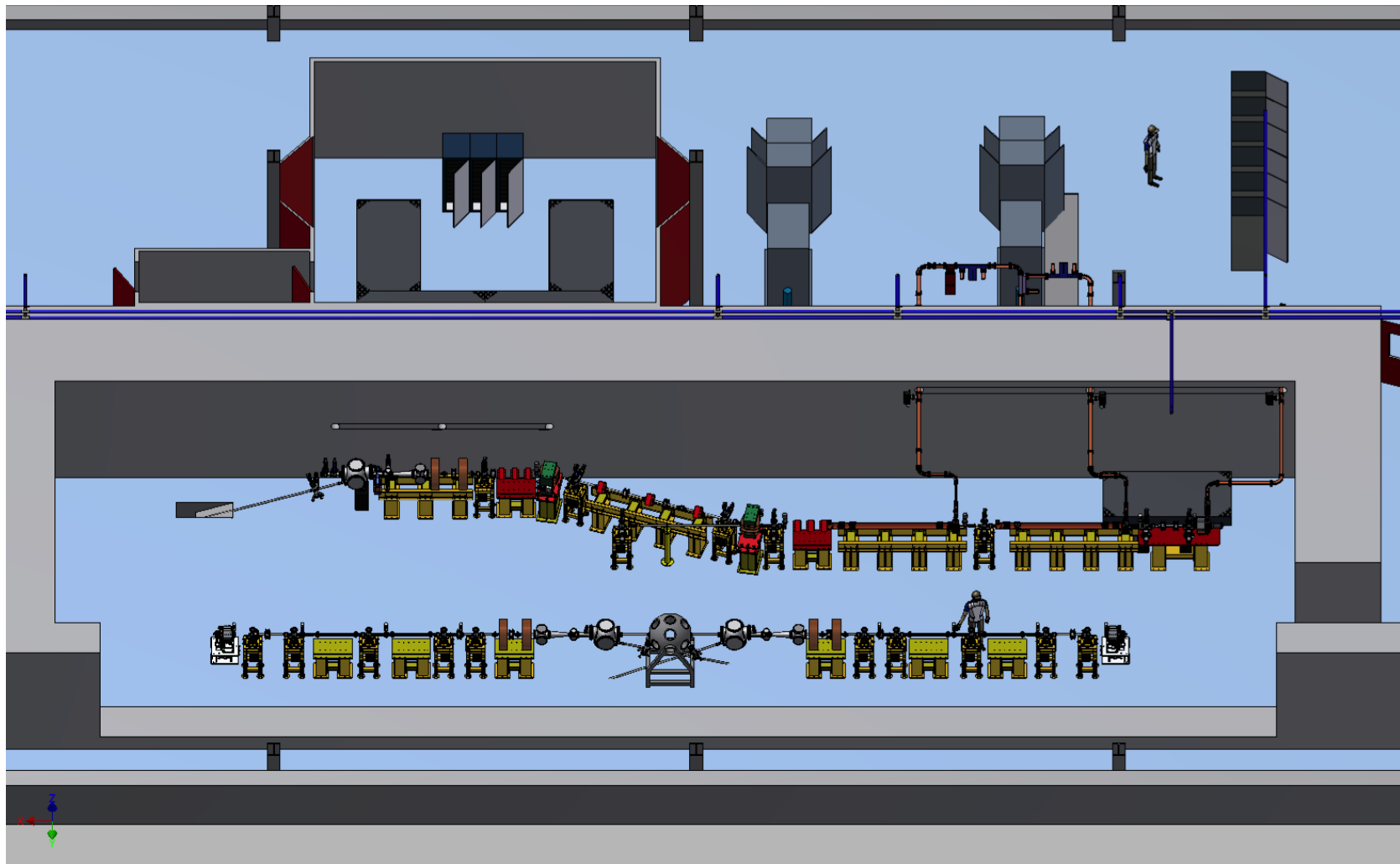
References

PVLAS

- Della Valle et al., PRD 90 (2014) 092003
- Della Valle et al., New J. Phys. 15 (2013) 053026
- Della Valle et al., Optics Express 22 (2014) 11570

Strong CP problem review

- Peccei, Nucl. Phys. B72 (1999) 3

Axion searches

- Van Bibber and Rosenberg, Phys. Today, Aug. 2006, 30
- Carosi et al., Contemp. Phys. 49 (2008) 281
- Redondo and Ringwald, Contemp. Phys. 52 (2011) 211

Pseudoscalar/scalar particle propagation in static fields

- Maiani, Petronzio & Zavattini, Phys. Lett. B 175 (1986) 359
- Gasperini, Phys. Rev. Lett. 59 (1987) 396

Seminal papers

- Okun, Zh. Eksp. Teor. Fiz. 83 (1982) 892
- Wilczek, PRL **58** (1987) 1799